

# Predictable Decadal Forcing of the North Atlantic Jet Speed by Sub-Polar North Atlantic Sea Surface Temperatures

Kristian Strommen<sup>a</sup>, Tim Woollings<sup>a</sup>, Paolo Davini<sup>b</sup>, Paolo Ruggieri<sup>c</sup>, and Isla R. Simpson<sup>d</sup>

<sup>a</sup>Department of Physics, University of Oxford

<sup>b</sup>Istituto di Scienze dell'Atmosfera e del Clima, Consiglio Nazionale delle Ricerche (CNR-ISAC), Torino

<sup>c</sup>Department of Physics and Astronomy, University of Bologna

<sup>d</sup>Climate and Global Dynamics Laboratory, National Centre for Atmospheric Research, Boulder CO

**Correspondence:** Kristian Strommen (kristian.strommen@physics.ox.ac.uk)

**Abstract.** It has been demonstrated that decadal variations in the North Atlantic Oscillation (NAO) can be predicted by current forecast models. While Atlantic Multidecadal Variability (AMV) in sea surface temperatures (SSTs) has been hypothesised as the source of this skill, the validity of this hypothesis and the pathways involved remain unclear. We show, using reanalysis and data from two forecast models, that the decadal predictability of the NAO can be entirely accounted for by the predictability of decadal variations in the speed of the North Atlantic eddy-driven jet, with no predictability of decadal variations in the jet latitude. The sub-polar North Atlantic (SPNA) is identified as the only obvious common source of an SST-based signal across the models and reanalysis, and the predictability of the jet speed is shown to be consistent with a forcing from the SPNA visible already within a single season. The pathway is argued to be tropospheric in nature, with the SPNA-associated heating extending up to the mid-troposphere, which alters the meridional temperature gradient around the climatological jet core. The relative roles of anthropogenic aerosol emissions and the AMOC at generating predictable SPNA variability are also discussed. The analysis is extensively supported by the novel use of a set of seasonal hindcasts spanning the 20th century and forced with prescribed SSTs.

## 1 Introduction

European winter weather is strongly influenced by the variability of the North Atlantic eddy-driven jet, and it is therefore of high societal value to predict this variability as far in advance as possible. Recent studies have shown that, remarkably, retrospective ensemble forecasts ('hindcasts') are now able to skillfully predict some components of the low-frequency variability of the winter jet at lead times of up to 10 years (Smith et al., 2019; Athanasiadis et al., 2020). However, the exact source of the predictable signal and mechanisms involved remain unclear, making it uncertain to what extent one can rely on this skill to remain for genuine decadal forecasts of the future. The aim of this paper is to try to clarify these points.

In Simpson et al. (2018), by considering a jet index based on zonal winds at 700hPa, it was shown that the decadal variability of the jet is much stronger in March than in the boreal winter months December, January, February (DJF). This late winter jet variability was argued to arise from the internally generated component of Atlantic Multidecadal Variability (AMV) in North Atlantic sea surface temperatures (SSTs), though the mechanisms were not elucidated; they also showed that models failed to

capture the connection. In alignment with the enhanced decadal variability, the observed connection between the AMV and the jet was shown to be far greater in March than during DJF. Nevertheless, Smith et al. (2019) and Athanasiadis et al. (2020) showed that skillful decadal forecasts of the DJF-averaged North Atlantic Oscillation (NAO) could be achieved, and the latter suggested that the skill appeared to be driven by the AMV. Both Smith et al. (2019) and Athanasiadis et al. (2020) emphasised an apparent ‘signal-to-noise paradox’ in these forecasts, mimicking the phenomenon observed for seasonal winter NAO forecasts (Scaife and Smith, 2018). This ‘paradox’ effectively says that the real world appears to be much more predictable than the forecast model thinks it is, with the model underestimating the response to forcing or the response to predictable boundary conditions on seasonal-to-decadal timescales relative to the unpredictable noise. A practical consequence of this behaviour is that models are likely underestimating the predictable component of decadal winter jet variability, suggesting that the results of Simpson et al. (2018) and Athanasiadis et al. (2020) are consistent with a hypothesis that the AMV is driving predictable decadal jet<sup>1</sup> variability from December through March. In fact, several studies have found that even the total decadal variability appears to be systematically underestimated in models (Kravtsov, 2017; Wang et al., 2017; Kim et al., 2018; Simpson et al., 2018; Bracegirdle, 2022).

Numerous studies have been conducted on the potential for air-sea coupling to generate links between the AMV and the jet, starting with the pioneering work of Bjerknes (1964). The decadal variability of the AMV itself has been hypothesised to be driven by a combination of the Atlantic Meridional Overturning Circulation (AMOC) (Bjerknes, 1964; Delworth et al., 1993; Kushnir, 1994), anthropogenic aerosols and other greenhouse gases (Booth et al., 2012; Bellomo et al., 2018; Robson et al., 2022), and stochastic atmospheric forcing (Hasselmann, 1976; Clement et al., 2015; O’Reilly et al., 2019). An excellent recent overview on these topics with more complete references can be found in Zhang et al. (2019). Different mechanisms have been put forward for how the AMV affects the jet, including the direct modulation of low-level baroclinicity and stationary waves by the North Atlantic SST anomalies (Kushnir, 1994; Msadek et al., 2011; Kushnir et al., 2002; Peings et al., 2016); forcing from the tropical Atlantic (Davini et al., 2015); and stratospheric pathways (Omran et al., 2014). However, the response in climate models to imposed AMV anomalies appears inconsistent and model dependent (Ruggieri et al., 2021), and the period of highly reliable observational data is short, making it challenging to distinguish between different hypotheses.

One major source of uncertainty in and across many studies is that the decadal variability is an average over several different processes occurring on different timescales, due to (a) the continuous nature of air-sea coupling and (b) the fact that the AMV pattern itself evolves over time, with the anomalies in the sub-polar North Atlantic (SPNA) arising first before propagating towards the tropical Atlantic (Zhang et al., 2019; Wills et al., 2019). This makes it difficult to attribute causality between atmospheric versus oceanic forcing and makes it unclear how to interpret the presence of multi-year lags in AMV-NAO links, such as the result that the AMV appears to force the NAO most strongly when leading by around 10 years (Peings and Magnusdottir, 2014a; Kwon et al., 2020). Furthermore, it becomes challenging to distinguish between the role played by particular regions in the Atlantic ocean, such as the sub-polar versus tropical North Atlantic. However, several studies have emphasised the importance of the SPNA in particular (Gastineau and Frankignoul, 2015; Woollings et al., 2015; Ortega et al., 2017; Wills et al., 2019), especially on longer timescales (Delworth et al., 2017).

---

<sup>1</sup> Since the NAO is largely describing the variability of the jet, we will conflate these without comment for the remainder of the paper.

In this paper, we make crucial use of two techniques to help address these challenges:

1. The separation of the eddy-driven jet into two components, corresponding to the speed and latitude of the jet.
2. The use of two seasonal hindcast ensembles, named ASF20C and CSF20C, spanning the period 1900-2010. ASF20C is forced with prescribed, observed boundary conditions (Weisheimer et al., 2017), while CSF20C is fully coupled (Weisheimer et al., 2020) (more details in Section 2.1).

The first point is motivated by the fact that the variability and sensitivity of the latitude and speed of the jet are very different. The jet latitude exhibits multimodality and considerable variability on seasonal timescales, but shows no significant variability on decadal timescales beyond white noise (Woollings et al., 2010, 2014). The jet speed, on the other hand, is approximately Gaussian across all timescales and exhibits robust decadal variability (Woollings et al., 2014). Furthermore, Baker et al. (2017) showed that the latitude and speed respond differently to thermal forcing, and Woollings et al. (2015) showed that the processes responsible for latitudinal shifts in the jet clearly differ from those responsible for changes to the jet speed. This means that analysis based on single indices which amalgamate the latitude and speed (such as the NAO index) may struggle to identify robust links between the jet and SST anomalies. This approach has also recently been taken in Marcheggiani et al. (2023) using a complementary set of decadal forecasts.

To motivate the second point, we note that existing decadal forecasts only go back to 1954 at the earliest, leaving them with a relatively small effective sample size once any low-pass filtering or decadal averaging has taken place. The period 1954 to present also does not adequately sample the variability associated with the AMV and the AMOC. There is therefore great value in extending the analysis back to 1900. While taking decadal averages of a seasonal hindcast obviously does not constitute an actual decadal *forecast*, it nevertheless turns out to be useful to think of it as being like a ‘nudged’ forecast, where both the atmospheric and oceanic state are being nudged back towards observations at the start of each winter (and moreover, for ASF20C, the SSTs are being forecasted perfectly). We will show that in fact the decadal variability reproduced by the seasonal hindcasts completely matches the predictable decadal variability of a genuine decadal forecast ensemble, justifying this perspective post hoc. This not only allows us to confidently use ASF20C/CSF20C to extend our analysis back to 1900, but also introduces two considerable benefits: the lack of coupling in ASF20C simplifies the question of causality between ocean and atmosphere, and the fact that the forecasts making up ASF20C/CSF20C only cover a single season simplifies the question of timescales.

We will show that on decadal timescales there is no predictability of the latitude of the jet, and that all the observed skill at predicting the winter NAO arises from the predictability of the *speed* of the jet. By comparing observations with the ASF20C/CSF20C seasonal hindcasts and the Decadal Prediction Large Ensemble (DPLE) decadal forecasts (Yeager et al., 2018), we argue that predictable forcing of the jet speed arises from SST anomalies in the SPNA. Furthermore, we argue that the predictable forcing occurring on decadal timescales arises as the accumulation of a smaller forcing taking place on seasonal timescales, with no need to consider multi-year lags. Finally, we argue that the response of the jet speed to SST anomalies in the SPNA can be understood simply as the adjustment of the jet to changes in the tropospheric meridional temperature gradient across the climatological jet core.

## 2 Data and Methods

### 2.1 Data

#### 2.1.1 ERA20C

95 We use the 20th century reanalysis dataset ERA20C, spanning 1890-2010, as our observational ‘truth’ (Poli et al., 2013). This reanalysis is constructed using a cycle of the Integrated Forecast System (IFS) forecast model, and is made up of consecutive 1-day forecasts with data assimilation. Due to differences in available observations between the beginning and end of the 20th century, the atmospheric component of ERA20C only assimilates surface pressure, in order to maintain coherence over the whole period. Both ocean and sea-ice boundary conditions come from the HadISST2.1.0.0 dataset (Rayner et al., 2003).  
100 Although it is known that the internal variability is underestimated in the early 20th century (Dell’Aquila et al., 2016), ERA20C constitutes a reasonable reference for the status of the North Atlantic climate.

#### 2.1.2 ASF20C and CSF20C

The ASF20C model data considered comes from an atmosphere-only seasonal hindcast experiment covering the 20th century (Weisheimer et al., 2017). A 51 ensemble member seasonal forecast is initialised every 1st of November from 1901 to 2010  
105 and allowed to run for 4 months, thereby producing a December-January-February (DJF) prediction for every year in this period. The model used is version CY41R1 of the IFS. Its spectral resolution is TL255, corresponding to roughly 80km grid spacing near the equator, with 91 levels in the vertical. The model is run in atmosphere-only mode with prescribed observed sea-surface temperatures (SSTs) with boundary conditions and initial conditions from ERA20C. Further details can be found in Weisheimer et al. (2017).

110 We will additionally make use of the CSF20C hindcast. This hindcast is identical to ASF20C except it is run with dynamic coupling between the atmosphere and ice/ocean, and is initialised using the coupled reanalysis CERA20C (Laloyaux et al., 2018). The configuration is described in Weisheimer et al. (2020) and is similar to the SEAS5 operational seasonal forecast at the European Centre for Medium-range Weather Forecasts (Johnson et al., 2019). The ocean model used is NEMO version 3.4 (Madec and the NEMO team, 2016), and the ice model is LIM2 (Fichefet and Maqueda, 1997). Both are run at a 1 degree  
115 horizontal resolution, with NEMO using 42 vertical levels.

#### 2.1.3 Decadal Prediction Large Ensemble (DPLE)

DPLE is made up of a suite of 40-member ensemble forecasts, each initialised on November 1st and run for 10 years. Forecasts are initialised every year from 1954 to 2015. The forecasts are run using CESM version 1.1, using the same model and component configuration as that used in the CESM1 large ensemble (Kay et al., 2015). The atmosphere component is version  
120 5 of the Community Atmosphere Model (CAM5: Hurrell et al. (2013)), with a horizontal resolution of around 1 degree and 30 levels in the vertical. The ocean component is version 2 of the Parallel Ocean Program (Danabasoglu et al., 2012) and the sea

ice model is version 4 of the Los Alamos National Laboratory (LANL) Community Ice Code (Hunke et al., 2010). Both are run at a 1 degree spatial resolution, with 60 vertical ocean levels. Further details can be found in Yeager et al. (2018).

To be consistent with CSF20C/ERA20C we restrict analysis to the overlapping period 1954-2010. When assessing the  
125 decadal forecast skill of DPLE, we always take averages over the entire 10-year period. For example, suppose we have a  
timeseries  $J$  made up of DJF averages of some quantity in reanalysis, and we want to assess the capacity of DPLE to predict  $\overline{J}$ ,  
where overline denotes the average across the 10 winters from November 1954 to February 1964. Then the DPLE forecast of  
 $\overline{J}$  is taken to be the ensemble mean over  $\overline{x_k}(k = 1, \dots, 40)$ , where the  $x_k$  are the 10-year forecasts initialised on November 1st  
1954, with  $k$  referring to ensemble member. By doing this for consecutive 10-year periods we obtain estimates of the decadal  
130 variability predicted by DPLE which we can correlate with the observed decadal variability.

Importantly, we do not perform any drift-correction of any kind in our analysis. The main goal of this paper is to understand  
how the atmosphere responds to decadal varying SSTs, and this can be assessed in DPLE irrespective of any drift taking  
place. Furthermore, it is not customary to de-drift seasonal forecasts, so no drift correction is done for ASF20C/CSF20C:  
not de-drifting DPLE therefore makes the analysis more directly comparable between the forecast products. For DPLE we  
135 will only ever consider two timescales: the response taking place in the first season or the 10-year mean across the whole  
forecast period. The drift taking place in the former is small, and the imprint of the drift in the latter is smoothed out by the  
large averaging-window. Finally, we note that Athanasiadis et al. (2020) found that robust decadal NAO forecast skill can be  
diagnosed in DPLE irrespective of whether drift-correction is carried out or not.

#### 2.1.4 EC-Earth3 data

140 We will make use of two piControl CMIP6 (500-year and 603-year long respectively) integrations from EC-Earth3 (Döscher  
et al., 2022). These simulations are atmosphere-ocean coupled runs with pre-industrial forcings. These simulations are specif-  
ically interesting owing to their large internal variability induced by an internally-driven centennial oscillation of the AMOC  
(Meccia et al., 2022), and we will use them to assess the potential role of the AMOC.

## 2.2 Methods

### 145 2.2.1 Metrics

The NAO index is computed as the leading EOF of daily deseasonalized DJF 500hPa geopotential height anomalies in the  
Euro-Atlantic sector 30-90N, 80W-40E. A seasonal cycle is estimated by taking the average daily NAO value, for each day in  
DJF, across all years available: this cycle is then removed. When computing the NAO index for ensemble forecast data, all the  
ensemble member data is used to compute the EOF, after which each members geopotential height field is projected onto the  
150 EOF pattern to obtain the individual NAO indices. The timeseries is not standardised further.

To compute indices of the jet speed and latitude, we follow the simplified methodology of Parker et al. (2019). Wind fields  
are first interpolated to a regular 1 degree grid. Daily DJF 850hPa zonal winds are then restricted to the region 15-75N, 60-20W  
and smoothed with a 5-day running mean. For any given day, the jet is said to be located at the latitude where the magnitude of

the zonally averaged winds in this region is maximum. The jet latitude on that day is precisely this latitude, while the jet speed  
155 is the magnitude of the maximum. As with the NAO, a seasonal cycle is removed.

An ‘SPNA’ index measuring SST variability in the sub-polar North Atlantic is also used extensively. This is defined as the  
DJF-averaged SSTs, averaged over the region 49-57N, 50-25W. The motivation for this precise choice is given in the main  
text. The results are not sensitive to small shifts in this region.

A more standard AMV index is also computed for comparison with the SPNA index. DJF SSTs in the North Atlantic domain  
160 0-70N, 80W-0W are detrended at every gridpoint; the first empirical orthogonal function of the resulting field is the standard  
AMV ‘horseshoe’ pattern, and we thus take the corresponding principal component to be our AMV index.

Note that we do not remove linear trends from any of these timeseries. The question of whether and how to isolate internal  
variability in the AMV and related timeseries is not entirely clear (Deser and Phillips, 2021) and trends in the SPNA and jet  
speed timeseries we primarily consider here are small (e.g. around -0.5% per year on average for the SPNA), with the decadal  
165 variability dominated by the oscillations characteristic of internal variability. Removing the trends is thus found to have no  
impact on the analysis (e.g. conclusions drawn concerning significance).

## 2.2.2 Statistics

Our default stance on significance testing is to explicitly specify a statistical model representing the null hypothesis, and then  
generate significance thresholds by making 10,000 random draws using the model; all tests carried out in this way are 2-sided.  
170 Because the motivation behind the choice of each statistical model depends on the situation at hand, we introduce each such  
model in the main text as and when it is required. However, we note that when modelling SSTs we generally make use of  
the ‘Fourier Phase Shuffling’ method (Ebisuzaki, 1997). This method can be loosely described as follows. First compute the  
Fourier transform of the timeseries of interest. Secondly, for each Fourier mode, replace the computed phase by a randomly  
chosen one. Third, convert the resulting Fourier series back to a timeseries. The resulting randomly generated timeseries is  
175 guaranteed to have the same autocorrelation (at all lags) and degrees of freedom as the original timeseries, which is important  
given the considerable autocorrelation present in the SST timeseries we will be examining. In particular, a null hypothesis  
modelling SSTs in this way will typically produce much stricter significance thresholds than those that model SSTs using an  
AR1, which only specifies the autocorrelation at lag 1.

## 3 Predictable jet variability in ASF20C and DPLE

### 180 3.1 Predictability of the jet speed and not the jet latitude

We first examine what low-frequency jet variability is skillfully reproduced by ASF20C. Figure 1 shows 10 and 30-year running  
means of the NAO, jet latitude and jet speed for ERA20C and the ASF20C ensemble mean. One aspect of the ‘signal-to-noise  
paradox’ is that the ASF20C ensemble mean standard deviation is considerably smaller than that of ERA20C: this can be seen  
here by comparing the magnitudes of the two  $y$ -axes, which highlight that the standard deviation in ERA20C is around 4-5

185 times greater than that of the ensemble mean. It can be seen that ASF20C skillfully reproduces decadal NAO variability across the entire period 1900-2010, with a correlation coefficient of  $\sim 0.4 - 0.7$  depending on the choice of smoothing: using the raw seasonal data gives a correlation of 0.21. The correlations obtained using 10-year smoothing closely match those reported in Smith et al. (2019) and Athanasiadis et al. (2020) using genuine decadal forecasts, suggesting that the decadal forecast skill they reported might extend all the way back to 1900. Figure 1 also clearly shows that ASF20C cannot skillfully reproduce  
 190 decadal jet latitude variability, but *can* skillfully reproduce decadal jet speed variability. Furthermore, if we regress out the (decadally averaged) ensemble mean jet speed from the ensemble mean NAO and correlate the residual with the observed NAO, we obtain  $\approx 0.1$  using 10-year averages and  $\approx -0.1$  using 30-year averages. Therefore, the majority of the skill that ASF20C has at reproducing decadal NAO variability is related to the jet speed. Figure A1 in the Supporting Information (SI) shows that, similarly, the coupled hindcast CSF20C has significant skill at predicting decadal variations in the speed but not  
 195 the latitude.

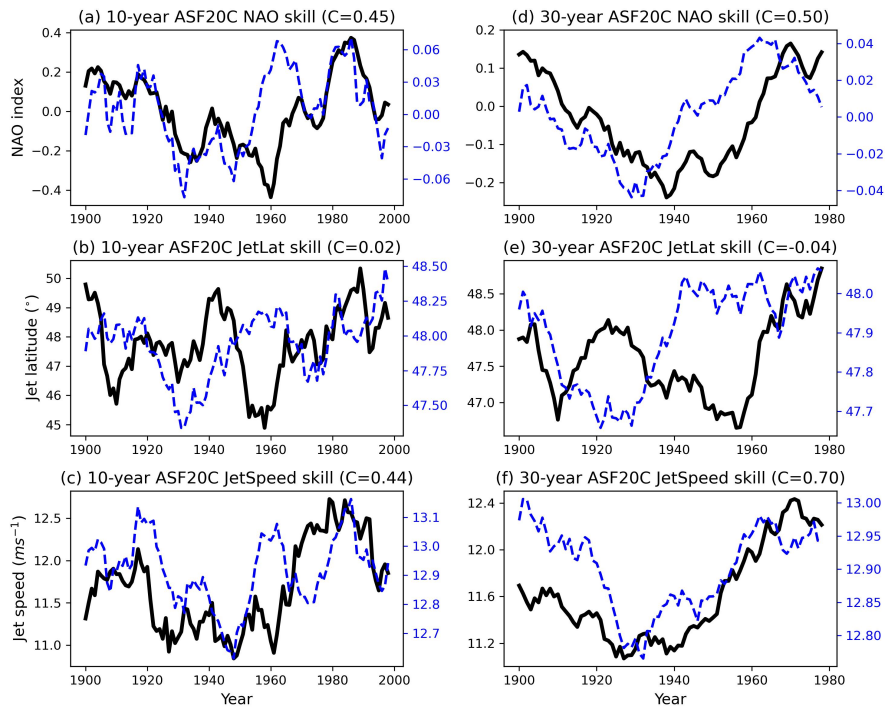


**Figure 1.** Timeseries of 10-year running DJF means of (a) the NAO, (b) the jet latitude, and (c) the jet speed. The same but with 30-year running means in (d), (e) and (f). The thick black curves are always ERA20C and the dashed blue curves are always the ASF20C ensemble mean. Note the different  $y$ -axes for the black and blue curves. The value  $C$  in each subplot is the correlation between the two timeseries.

Figure 2 shows that the same conclusion is true for the DPLE forecasts: there is no apparent predictability of decadal shifts in the jet latitude, but high skill at predicting shifts in the jet speed. Note that taking 30-year means is much less sensible for DPLE, given its shorter coverage of 56 years, but these are included anyway for direct comparison with Figure 1.

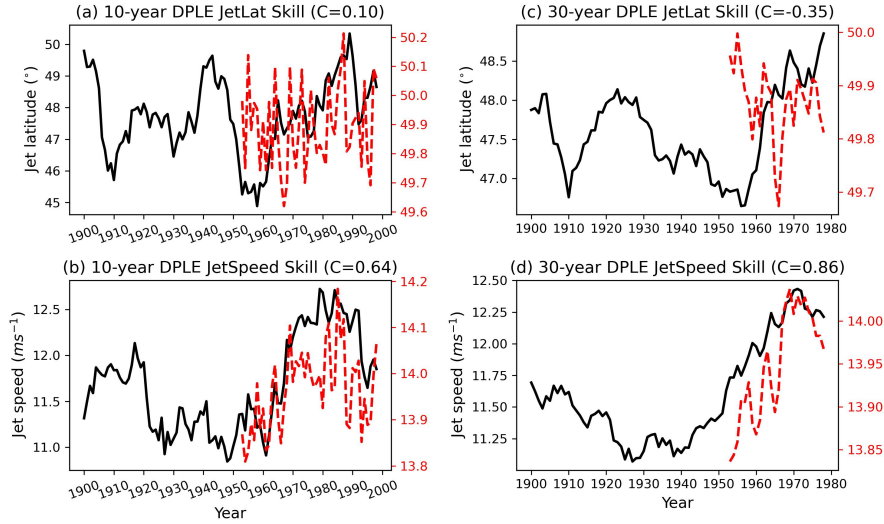


**Figure 2.** Timeseries of 10-year running DJF means of (a) the jet speed, and (b) the jet latitude. The same but with 30-year running means in (c) and (d). The thick black curves are always ERA20C and the dashed red curves are always the DPLE ensemble mean. Note the different  $y$ -axes for the black and red curves. The value  $C$  in each subplot is the correlation between the two timeseries.

<b>JetSpeed correlations</b>	10 year smoothing	30 year smoothing
Corr(ERA20C, ASF20C)	0.44	0.70
10% significance threshold	$\pm 0.42$	$\pm 0.70$
5% significance threshold	$\pm 0.48$	$\pm 0.80$
Corr(ERA20C, DPLE)	0.64	0.86
10% significance threshold	$\pm 0.62$	$\pm 0.80$
5% significance threshold	$\pm 0.71$	$\pm 0.85$

**Table 1.** DJF jet speed correlations between different data sets at different levels of smoothing. Significance thresholds assume a null hypothesis of the interannual jet speed timeseries being uncorrelated white noise.

How significant are the jet speed correlations reported in Figures 1 and 2? The 1-year jet speed autocorrelation is  $\approx 0.0$  for all three data sets, and we are therefore justified in assuming a null hypothesis of the DJF jet speed as being white noise. The approximate Gaussianity of the jet speed distribution has been previously noted (Woollings et al., 2010; Parker et al., 2019). By simulating 10,000 randomly generated DJF jet speed timeseries for each data set, taking 10 or 30-year running means and then computing correlations, we build up a distribution of correlations that can be obtained by chance. Note that taking running means will automatically introduce considerable autocorrelation to the resulting timeseries. Table 1 summarises the result of this significance testing. This shows that for ASF20C, whether considering 10 or 30 year smoothing, the decadal jet speed correlations are only significant to within  $p < 0.1$  and not  $p < 0.05$ : the same is true for CSF20C (see Figure A1). For DPLE,



the conclusion is the same except that the correlations using 30-year smoothing appear to be significant also with  $p < 0.05$ . However, as cautioned already, the small effective sample size here means that this level of confidence is probably not justified. The jet latitude correlations are never significant with respect to a similar null hypothesis, including the relatively large negative correlation emerging for 30-year jet latitude variability in DPLE ( $C = -0.35$ ).

Our results here contrast somewhat with those of Smith et al. (2019) and Athanasiadis et al. (2020), which both report statistically significant decadal NAO forecasts with  $p < 0.05$ . However, their significance tests differ from ours, and the smoothing they use is also very close, but not identical, to the 10-year running means we use. Table 1 shows that the 10-year ASF20C and DPLE jet speed correlations sit neatly between the bounds of the 5 and 10% significance thresholds, and it is therefore plausible that these differences can explain why they report a  $p$ -value less than 0.05 and we do not. For this article, we will assume that ASF20C and DPLE really do have significant skill at predicting decadal variations in the jet speed.

### 3.2 Predictable atmospheric signals appear on interannual timescales

The similar behaviour of ASF20C and DPLE suggests that the extra information provided to ASF20C (the correct climate state every November 1st and the correct SSTs at all times) is not adding any extra jet speed skill beyond what is expected from an actual free-running, coupled decadal forecast. We interpret this as evidence for the assertion that the signals responsible for predictable decadal shifts in the jet speed are fully represented in ASF20C, and we will from now on assume that this is the case; we return to this point and alternative hypotheses later. Our assumption has two important consequences.

Firstly, since each of the 109 ASF20C winter forecasts only knows about the initial conditions and boundary forcings of the season in question, the sources of predictable decadal jet speed forcing must be present in their entirety within a single winter season. Put differently, since the atmospheric variability in ASF20C is generated by forecasts of a single season, any decadal variability ASF20C generates must arise due to atmospheric variability taking place within single seasons, even if this variability is ultimately forced by variables (e.g. SSTs) evolving on slower timescales. In particular, the predictable atmospheric signals, and the mechanisms involved, do not seem to inherently involve multi-year lags between the ocean and atmosphere or multi-year feedbacks within the atmosphere. Secondly, since the ASF20C forecasts are uncoupled, the forcing being exerted on the jet by the SSTs does not essentially depend upon atmosphere-ocean coupling, in the sense that no within-season-feedbacks are necessary. To the extent that there is any causal interaction between the SSTs and the atmosphere in ASF20C, it must purely be from the former to the latter. In the sections that follow we will make use of these two points repeatedly to simplify the analysis and reasoning.

We emphasise straight away that while two-way surface coupling appears to not be required to reproduce the low frequency jet speed variability, missing or deficient coupling may play a role in generating the ‘signal-to-noise paradox’, as suggested in Scaife and Smith (2018). It is also likely that atmosphere-ocean coupling plays a role in generating the decadal timescale SST variability.

## 4 Sources of predictability from sea surface temperatures

The midlatitude troposphere broadly speaking has a decorrelation timescale of about 2 weeks (Judt, 2020), and this is also true  
240 for the daily jet speed index (not shown). This strongly suggests that the skill in both ASF20C and DPLE cannot be explained  
by the persistence of atmospheric initial conditions, and is rather a result of forcing from some other slow timescale process.  
Due to the considerable body of work emphasising the importance of SSTs in generating forecast skill, we make the assumption  
here that decadal jet speed skill is a result of SST forcing. The validity of this assumption is discussed in Section 7.1.

### 4.1 Sub-polar North Atlantic SSTs as a common signal across observations and forecasts

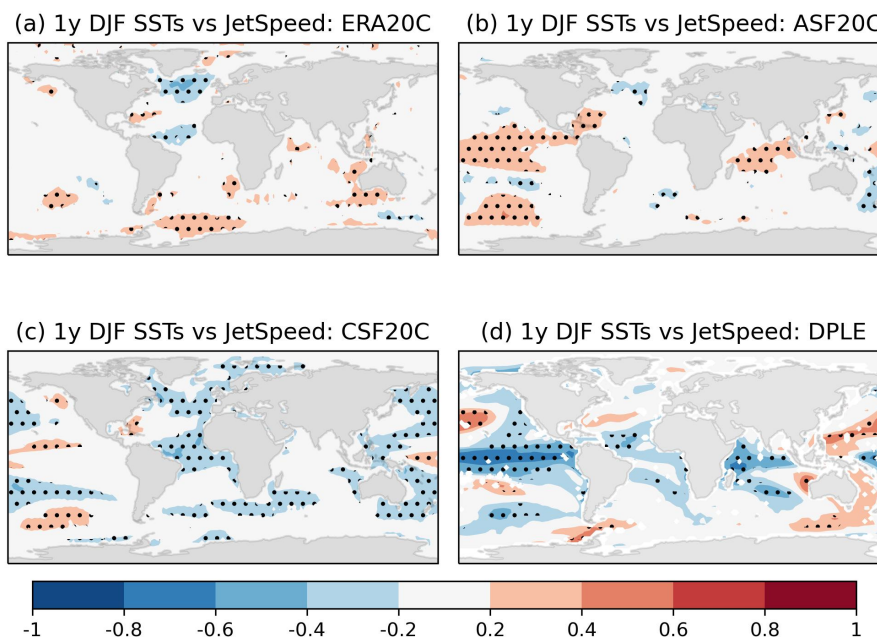


**Figure 3.** Correlations between the interannual DJF JetSpeed timeseries and DJF SSTs at each gridpoint. In (a) ERA20C, (b) ASF20C (c) CSF20C, (d) DPLE. Stippling indicates significance ( $p < 0.05$ ): see main text for details of the null hypothesis. The period considered is 1954-2010 for DPLE and 1900-2010 otherwise.

245 In order to locate potential sources of skill in SSTs, we compute correlations of the winter jet speed against winter SSTs at  
every gridpoint. Because of our conclusion that these sources must be visible already on seasonal timescales (see Section 3.2),  
we do this using both the raw DJF timeseries as well as timeseries obtained by applying a 10-year running mean. Potential  
sources of skill are then assumed to correspond to regions of non-zero correlations that are common to ERA20C, ASF20C,  
CSF20C and DPLE across both interannual and decadal timescales. While it is of course possible that the locations of signals  
250 differs somewhat across the datasets (e.g. due to biases in both the mean state and trends across the forecast models), the

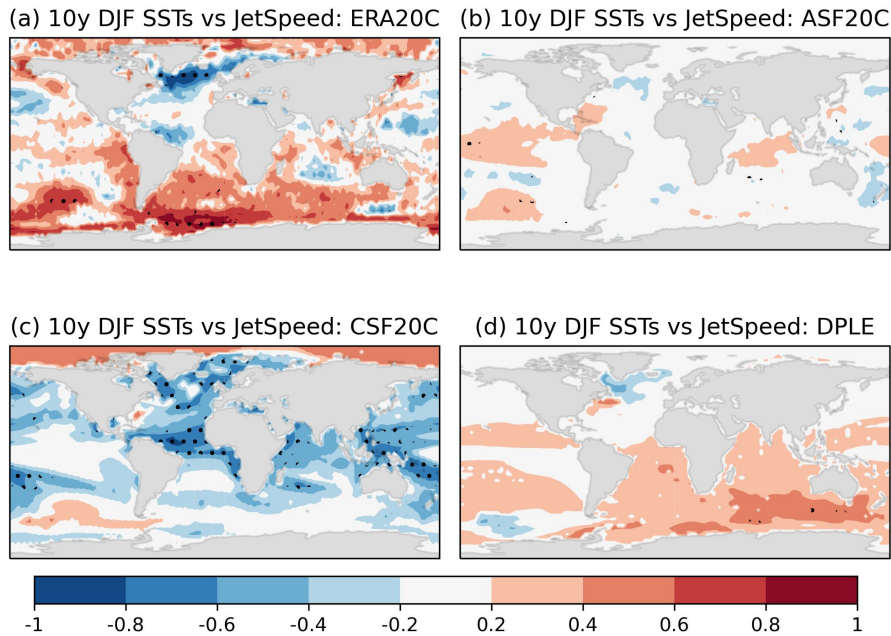


**Figure 4.** Correlations between 10-year running means of the DJF JetSpeed timeseries and DJF SSTs at each gridpoint. In (a) ERA20C, (b) ASF20C (c) CSF20C, (d) DPLE. Stippling indicates significance ( $p < 0.05$ ): see main text for details of the null hypothesis. The period considered is 1954-2010 for DPLE and 1900-2010 otherwise.

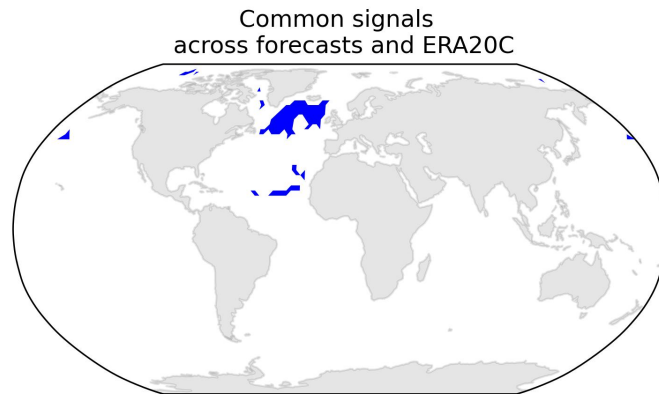


**Figure 5.** Gridpoints where the correlations in all eight subplots of Figures 3 and 4 have the same sign. Blue (red) gridpoints correspond to ones where the shared sign is negative (positive). Gridpoints where the sign is not consistent across all subplots have been left blank.

simplest - and more physically sound - possibility is that the signals are identical across the datasets, so we consider this possibility first.

Figure 3 shows gridpoint correlations for ERA20C, ASF20C, CSF20C and DPLE at interannual timescales, while Figure 4 shows gridpoint correlations of 10-year running means. Stipling indicates significance ( $p = 5\%$ ), where for interannual timescales the null hypothesis models the jet speed as white noise and models gridpoint SSTs using the Fourier phase shuffle method; on decadal timescales both the jet speed and SSTs are modelled using the phase shuffle method. At each gridpoint 1000 randomly generated samples from the null hypothesis are drawn in order to compute significance thresholds. Searching for commonalities across all the 8 subplots by eye quickly highlights the SPNA. Already just comparing Figures 3(a) and (b) makes this clear. A comparison with CSF20C and DPLE corroborates this, and furthermore seems to rule out signals from both the tropical Pacific, tropical Atlantic and Indian ocean, since the correlations are opposite in sign between ASF20C/CSF20C and DPLE in these regions.

To justify this visual inspection more objectively, we have in Figure 5 highlighted the gridpoints for which all the four data sets exhibit interannual and decadal timescale correlations with the same sign. This makes it clear that the SPNA is the only region where spatially coherent correlations of the same sign can be found. Figures 3 and 4 show that the correlations in the SPNA region are statistically significant in 5 out of 8 subplots, including in ERA20C across both timescales. While Figure 5 shows a narrow strip of shared negative correlations in the tropical Atlantic, these correlations are not significant in ASF20C on any timescale and are not significant in ERA20C on decadal timescales. The correlations in this region are also close to 0 in magnitude in ASF20C on interannual timescales and DPLE on decadal timescales ( $\approx -0.05$  on average in both cases). Only in the SPNA are correlations of appreciable magnitude ( $< -0.2$ ) found in all data sets on all timescales. Furthermore, and crucially, the coupled DPLE forecasts have considerable skill at predicting decadal SST variability in the SPNA region but not in the tropical Atlantic (Yeager et al., 2018; Yeager, 2020).

The SPNA thus emerges as a common region of interannual-to-decadal correlations between SSTs and the jet speed across ERA20C, ASF20C, CSF20C and DPLE, and appears to be the only such common region. We interpret this as strong evidence for the importance of the SPNA in driving decadal jet predictability. We therefore define an SPNA timeseries as the DJF averaged SSTs across the domain 49-57N, 50-25W. This box was chosen because it encloses almost precisely the negative correlations highlighted in Figure 3(c) in the sub-polar region. The remainder of the analysis we carry out is not sensitive to even moderately large shifts in the definition of this box, as long as the box roughly belongs to the region highlighted in Figure 5. Other differences between the datasets seen in Figures 3 and 4, while interesting, do not seem relevant to the study at hand, and so are not discussed.

It is worth mentioning the phenomenon of false discovery rates, namely the fact that if one looks for correlations across sufficiently many predictors then some are bound to be significant by chance. This effect would a priori be expected to be high when considering correlations across thousands of gridpoints with high spatial autocorrelation. However, based on the results and discussion of previous sections, we are now assuming that (a) there is decadal forecast skill which needs to be explained and (b) that this skill comes from the SSTs. A rejection of any and all gridpoint correlations as ‘false discoveries’ would be directly counter to this assumption, and is therefore not done. The discovery of a region of correlations common across 4 data sets on the other hand can be seen as providing additional evidence towards our assumption.

SPNA vs JetSpeed	Raw	10 year smoothing	30 year smoothing
ERA20C	<b>-0.45</b>	<b>-0.88</b>	<b>-0.97</b>
ASF20C	<b>-0.24</b>	-0.41	-0.68
CSF20C	<b>-0.27</b>	<b>-0.57</b>	-0.70
5% significance threshold	$\pm 0.19$	$\pm 0.56$	$\pm 0.84$
DPLE	-0.13	-0.28	-0.88
5% significance threshold	$\pm 0.29$	$\pm 0.81$	$\pm 0.92$

**Table 2.** Correlations between DJF averaged SPNA SSTs and DJF averaged jet speed at different levels of smoothing. The 5% significance thresholds shown use the null hypothesis described in the main text. Significant correlations are highlighted in bold.

## 4.2 Significance of the SPNA-JetSpeed link

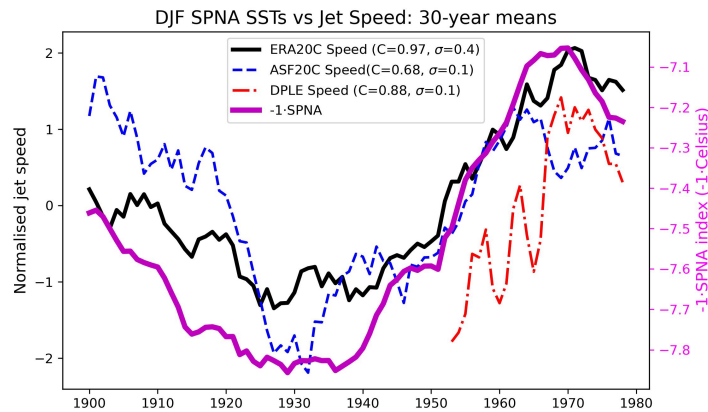


**Figure 6.** Timeseries of 30-year running means of ERA20C SPNA SSTs (thick purple: the sign has been flipped for visual convenience), ERA20C jet speeds (thick black), ASF20C ensemble mean jet speeds (dashed blue) and DPLE ensemble mean jet speeds (dashed red). The values of  $C$  in the legend indicate the correlation between the jet speed timeseries and the relevant SPNA timeseries, and the values of  $\sigma$  indicates the standard deviations of the jet speed timeseries. Note the different  $y$ -axes for the jet speed and SPNA timeseries. The jet speed indices have all been normalised to have mean 0 and standard deviation 1.

Table 2 summarises the correlations between SPNA SSTs and jet speed for the different datasets across different timescales. Figure 6 visualises the 30-year running mean timeseries: the sign of the SST index has been flipped for visual convenience. To generate the 5% significance threshold reported in the table, we assume a null hypothesis that the jet speed and SPNA are uncorrelated random variables. The interannual jet speed timeseries is modelled as a normal distribution with no memory across years, as before. To create synthetic SPNA timeseries, we apply the Fourier phase shuffle method to the interannual SPNA timeseries, in order to generate random draws that preserve the considerable autocorrelation. By correlating 10,000 such

synthetic timeseries, along with those obtained by applying a 10 or 30-year smoothing, we can then numerically estimate the  
295 5% significance threshold. Note that the confidence intervals for ERA20C, ASF20C and CSF20C were found to be almost  
identical, so we only report a single confidence interval encompassing all three, obtained by taking the average across the three  
individual intervals.

The correlation between SPNA and the jet speed is highly significant in ERA20C for all timescales considered here, suggest-  
ing a robust physical link between these quantities. Both ASF20C and CSF20C have significant correlations on the interannual  
300 timescale, and CSF20C also for 10-year timescales. The other correlations obtained do not pass the threshold. Of course, the  
lack of consistent statistical significance at 5% does not mean the physical link in ERA20C is not simulated by the forecast  
models, only that these correlations would not be sufficient to establish such a link when viewed in isolation. As emphasised in  
Shepherd (2021), it is crucial to include physical reasoning and prior knowledge when drawing conclusions about significance.  
We return to this, and the question of causality, in the Discussion section.

## 305 5 Pathways and timescales

### 5.1 The tropospheric pathway from sub-polar North Atlantic SSTs to the jet speed

When studying the impact of imposed temperature anomalies on the jet in a dry model, Baker et al. (2017) argued that much  
of the response could be understood simply in terms of changes to the meridional temperature gradient. This suggests a  
simple explanation for why the SPNA forces the jet in keeping with the analysis of Woollings et al. (2015): anomalously  
310 cold SSTs in the SPNA cool the atmosphere aloft, thereby strengthening the local meridional temperature gradient around  
the jet, causing an intensification of the eddies and thereby an increased jet speed. Similarly for warm anomalies but with the  
opposite sign. To strengthen the case for this pathway, Figure 7 shows the vertical extent of the anomalies associated with  
SPNA SSTs in ERA20C, by correlating November SPNA SSTs with zonally averaged (a) temperatures and (b) zonal winds  
at different pressure levels: the averaging is done over longitudes 60W-20E. Significance at 5% (indicated by stipling) uses  
315 a null hypothesis which models the SPNA using the Fourier phase shuffle method and temperatures/winds as white noise.  
Figures (c) and (d) show the same but using DJF means. Figures 7(a) and (c) suggest that temperature anomalies do not remain  
confined to the surface, but extend up to around 300hPa, making the robust impact on the jet seen in Figure 7(b) plausible. For  
completeness, the reverse link from the jet speed to temperatures and winds is shown in Figure 8. Figure 8(a) shows that the  
temperature anomalies associated with the jet are maximal in the mid-troposphere. The temperature anomalies associated with  
320 the SPNA (Figure 7(a) and (c)) project well onto the jet pattern, but is maximal at the surface. Comparing Figures 7(d) and  
8(b) confirms that the association between the SPNA and the zonal winds projects onto the jet speed signature.

Detailed analysis of the tropospheric response to an SST anomaly in the North Atlantic, such as in Deser et al. (2007), show  
that the response generally proceeds in two stages. To begin with, the induced anomaly is baroclinic in nature and localised  
to the heat source. In the second stage the baroclinic anomalies are removed by eddy heat and momentum transport, leading  
325 to a relatively barotropic structure with a more hemispheric scope. Figure 7 shows that in DJF, the structures are relatively

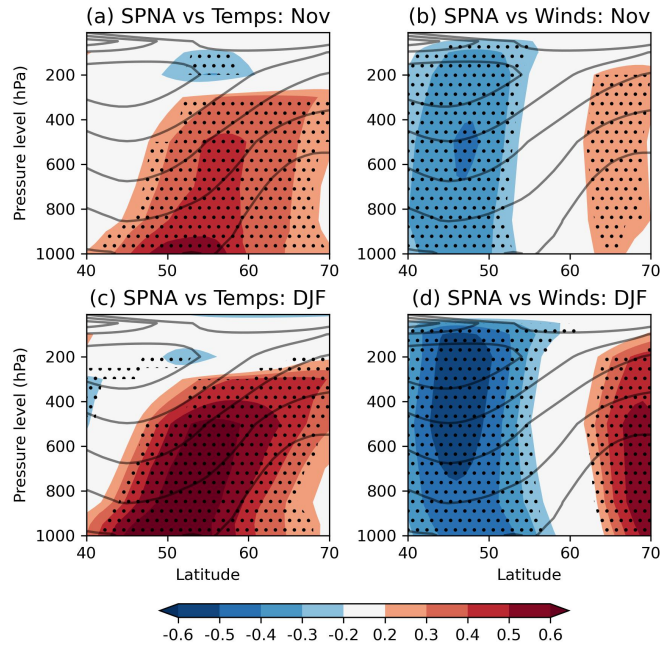


**Figure 7.** Correlations in ERA20C between SPNA SSTs and (left column) zonally averaged air temperatures at different pressure levels; (right column) zonally averaged zonal winds at different pressure levels. November averages are used in (a) and (b), while DJF averages are used in (c) and (d). The period 1900-2010 is used. The climatological zonal winds are shown in grey contours. Stippling indicates significance ( $p = 5\%$ ): see main text for details.

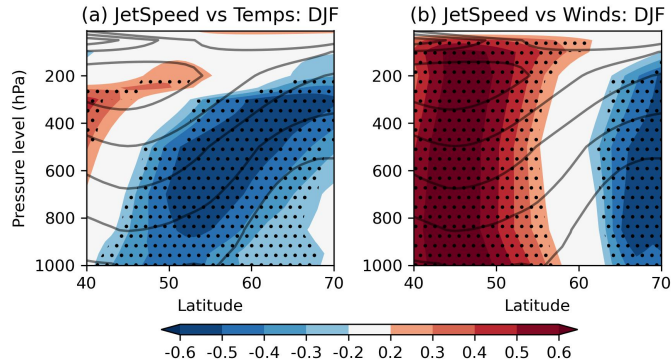


**Figure 8.** Correlations in ERA20C between jet speeds and (a) zonally averaged air temperatures at different pressure levels; (b) zonally averaged zonal winds at different pressure levels. DJF averages are used in both. The period 1900-2010 is used. The climatological zonal winds are shown in grey contours. Stippling indicates significance ( $p = 5\%$ ) with respect to a two-tailed t-test.

barotropic in nature, consistent with this tropospheric pathway having taken place. Note that this approximately barotropic structure is also visible when plotting regression coefficients instead of correlations (not shown).

To further test the importance of the tropospheric heating anomalies over the SPNA, we will compute a crude estimate of what ERA20C jet speed anomalies are expected purely from SPNA variability using geostrophic wind balance. Concretely, we  
 330 will estimate the jet speed variability expected from the following assumptions:

- (1) That the local meridional temperature derivative at the jet core can be completely approximated using the difference in temperatures between the jet core and the SPNA region (which sits on the northern flank of the jet). In particular, we assume that the gradient between the southern flank and the jet core does not contribute to the local derivative.
- (2) That the only air temperature variability which takes place in the period 1900-2010 is that in the atmosphere above the  
 335 SPNA. In particular, temperatures above the jet core are assumed to be constant in time.

We emphasise that these are strictly stronger assumptions than standard geostrophic balance, and it is therefore not obvious, a priori, that these assumptions should suffice to accurately reconstruct jet speed variability.

To proceed, we define a region labeled ‘South’ by 35-43N, 75-40W, and a region labeled ‘North’ using the same domain as the SPNA. The ‘South’ region is chosen because it roughly encompasses the climatological core of the jet in ERA20C (not  
 340 shown). We then assume a constant layer-thickness between 1000 and 300hPa, where 300hPa is the upper limit of the heating associated with the SPNA, as seen in Figure 7(c). Let  $\hat{T}_N$  and  $\hat{T}_S$  denote the layer-averaged DJF air temperature between 1000 and 300hPa in the North and South regions. By regressing our SPNA SST timeseries against  $\hat{T}_N$ , we obtain the SPNA-driven component which we denote by  $\hat{T}_N(SPNA)$ . We let  $[\hat{T}_S]$  denote the average of  $\hat{T}_S$  across all years 1900-2010. The timeseries of the difference  $\hat{T}_N(SPNA) - [\hat{T}_S]$  thereby roughly measures the layer-averaged meridional temperature gradient across  
 345 the jet core purely associated with SPNA SST variability. Given our two assumptions, geostrophic balance with a constant layer-thickness now relates this gradient to the zonal winds  $U_{jet}$  in the jet core according to

$$U_{jet} = -\frac{R}{f} \cdot \log(1000/300) \cdot \frac{1}{dy} (\hat{T}_N(SPNA) - [\hat{T}_S]), \quad (1)$$

where  $R = 287.05 (J kg^{-1} K^{-1})$  is the gas constant,  $f = 1 \times 10^{-4} (rad/s)$  is the approximate midlatitude Coriolis parameter, and  $dy = 2.553 \times 10^6$  metres. Here we have used that 1 degree latitude is roughly 111km. The  $U_{jet}$  anomaly timeseries is  
 350 compared to the jet speed timeseries for ERA20C in Figure 9 using 30-year averages. They not only correlate extremely well ( $C = 0.97$ ), but the magnitudes of the anomalies are also almost identical. The raw means of the two timeseries were found to differ, with the JetSpeed mean being around 25% larger. This is likely due to both the the crude estimate of the local derivative we made use of, and the fact that  $U_{jet}$  is an average across multiple layers, unlike JetSpeed, which is measured at the 850 hPa level only. Nevertheless, we conclude that the decadal jet speed variability of ERA20C can be accounted for purely by  
 355 tropospheric temperature anomalies associated with the SPNA<sup>2</sup>.

<sup>2</sup>We remark that we also found that around 60% of the CMIP5/6 intermodel spread in climatological jet speeds could be accounted for by these tropospheric anomalies (not shown), further emphasising the importance of this region.



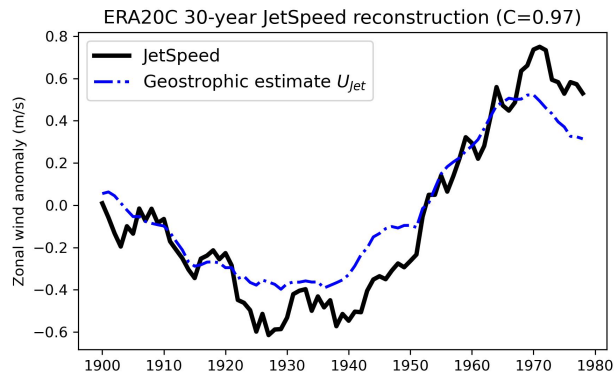


**Figure 9.** Black curve: 30-year averaged ERA20C DJF jet speed anomalies. Blue dashed curve: 30-year averages of the ERA20C  $U_{jet}$  anomaly timeseries, which roughly estimates the anomalous zonal wind variability associated with SPNA-induced changes to the meridional temperature gradient assuming geostrophic balance (see main text for details). The value  $C$  denotes the correlation coefficient between the two timeseries.

We emphasise that the specific nature of the fast timescale processes responsible for bringing the jet into geostrophic balance, including the role of moist processes, is actively studied (Fuchs et al., 2023; Schemm, 2023), and we do not shed any further light on these. The above analysis simply says that if the SPNA is heating the atmosphere aloft then geostrophic balance effectively forces the jet speed to exhibit the decadal variability we observe.

## 360 5.2 Decadal timescale forcing as the accumulation of seasonal timescale forcing

In Section 3.2, we argued that the presence of skill in ASF20C implies that predictable jet speed variability is a result of forcing from the boundary conditions taking place already within a single season. Having now argued that this forcing is coming from SPNA SSTs, it remains to test whether the forcing exerted by the SPNA on the jet taking place on seasonal timescales suffices to explain decadal timescale correlations seen in Table 2. That is, we want to test the following hypothesis: that the jet’s response  
 365 to the SPNA is established within a single season, and that the decadal signal seen in the jet speed arises purely from decadal power in the SSTs, without the need to invoke slower multi-annual-to-decadal timescale processes or feedbacks.

To test this, we model the SPNA-JetSpeed system as follows. For a given dataset, we perform a linear regression of the interannual SPNA timeseries against the interannual JetSpeed timeseries to get

$$\text{JetSpeed} = a \cdot \text{SPNA} + b + \epsilon \quad (2)$$

370 for some constants  $a, b$  and a noise term  $\epsilon$  which is normally distributed with mean 0. We then generate a random, synthetic timeseries of DJF SPNA using the Fourier phase shuffle method, as in the previous subsection. A corresponding JetSpeed timeseries is then obtained using the linear relationship just derived; the synthetic jet speed thus relies only on the simultaneous synthetic SPNA in that season. We then take 10 and 30-year running means of these synthetic DJF timeseries and compute the

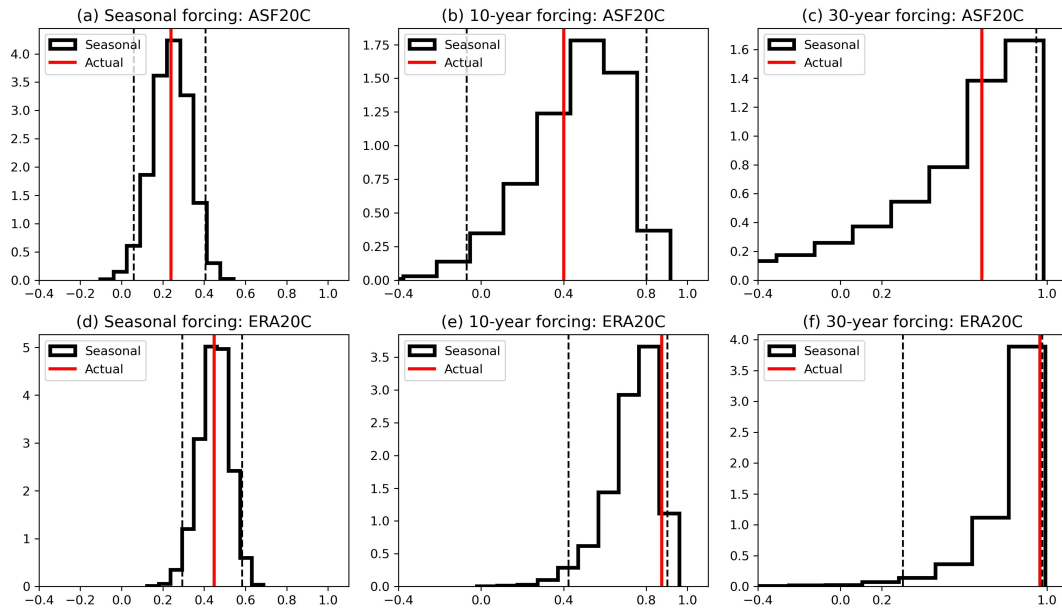


**Figure 10.** Histograms of the SPNA-JetSpeed correlations expected by chance from the seasonal timescale link, (a) and (d); taking 10-year averages of the seasonal link, (b) and (e); taking 30-year averages of the seasonal link, (c) and (f). See main text for details. The top row uses data fitted to ASF20C and the bottom to ERA20C. In each subplot the red line indicates the actual correlation found in that dataset, and the dashed lines indicate the 95% confidence interval. The histograms are normalised so that the area underneath is 1.

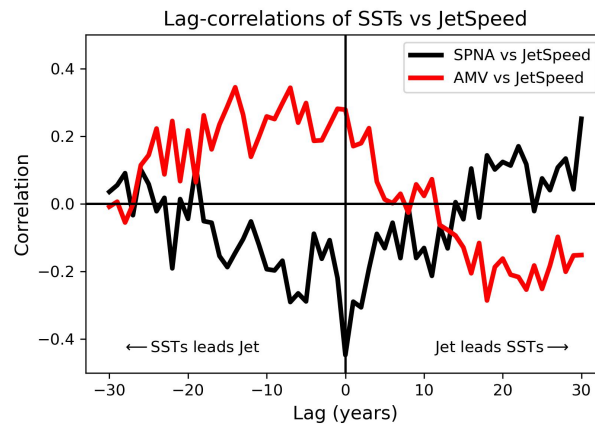


**Figure 11.** Lag correlations of DJF SPNA (black) and AMV (red) against JetSpeed timeseries in ERA20C. Negative lags correspond to SSTs leading the jet, and positive lags to SSTs lagging the jet. The period covered is 1900-2010.

375 correlations between them. By repeating this procedure 10,000 times we can assess what decadal timescale correlations are expected from taking running means of the interannual SPNA-JetSpeed link.

The result of this for ASF20C is summarised in Figures 10(a), (b) and (c). The synthetic seasonal timescale correlations (Figure 10(a)) capture the actual seasonal correlation by construction. After taking running means, the distribution of synthetic correlations becomes notably skewed. For both 10 and 30-year running means (Figure 10(b) and (c)), the observed correlation is still comfortably within the 95% confidence interval of the synthetic correlations. The same analysis for ERA20C is shown in  
380 Figures 10(d), (e) and (f). The observed 10 and 30-year correlations are closer to the upper threshold here, but still fall within. This implies that the decadal timescale correlations of ASF20C and ERA20C can be completely explained by the interannual SPNA-JetSpeed link, as hypothesised.

We emphasise that we are not suggesting the SPNA variability is purely interannual, but that the connection between the SPNA and the atmosphere occurs within the span of a single season. The same conclusion can be seen to hold for CSF20C by  
385 comparing Table 2 with Figure 10; we also verified the analysis using the shorter DPLE (not shown). To further support this point, Figure 11 shows lag correlations of the jet speed in ERA20C against the SPNA timeseries (black curve). The correlations peak at lag 0 and diminish towards 0 for increasingly negative lags, consistent with an instantaneous forcing from a (decadally varying) SPNA which slowly diminishes over time. The comparison with the AMV lag-correlations (red curve in Figure 11) will be discussed in Section 7.3.

## 390 **6 Drivers of decadal SST variability and their link to the jet speed**

We have highlighted SSTs in the SPNA as the main source of decadal predictability of the jet speed. Identifying the drivers of SPNA variability and their relation to jet speed variability is thus important for understanding how reliable forecast skill is likely to be in the future. A comprehensive examination of this using the jet speed framework goes beyond the scope of the paper. Here we limit ourselves to only considering two key potential drivers: anthropogenic sulphate aerosols and the AMOC.

### 395 **6.1 The role of sulphate aerosols**

The question of how aerosols affect North Atlantic SSTs is still actively debated, and could include the role of both direct radiative adjustments local to the region, as well as more indirect impacts from upstream emissions (Booth et al., 2012; Robson et al., 2022). Here we will only consider the hypothesis put forth by Robson et al. (2022), due to it being based on a large multimodel ensemble, unlike most other studies. In their study, they argued that sulphate aerosol emissions over the eastern  
400 part of North America led to a cooling of surface temperatures there, and that this cool air was then advected over the North Atlantic, thereby cooling the SSTs and ultimately modulating the AMOC. The possible direct impacts of emissions over the SPNA region itself will not be considered, since the emissions are generally very low in this region.

ERA20C, ASF20C and CSF20C all share the same prescribed aerosol emissions, namely those used in CMIP5 (Lamarque et al., 2010). The climatological SO<sub>4</sub> emissions are shown in Figure 12(a), showing a clear concentration of emissions over the  
405 eastern North American region. To study the impact of these emissions on the SPNA and jet speed, we define an SO<sub>4</sub> timeseries by averaging the emissions over the box 30-45N, 100-75W. This box is visualised in Figure 12(a) and approximately covers the eastern North American continent. This timeseries is compared to the 10-year averaged SPNA SSTs and ERA20C jet

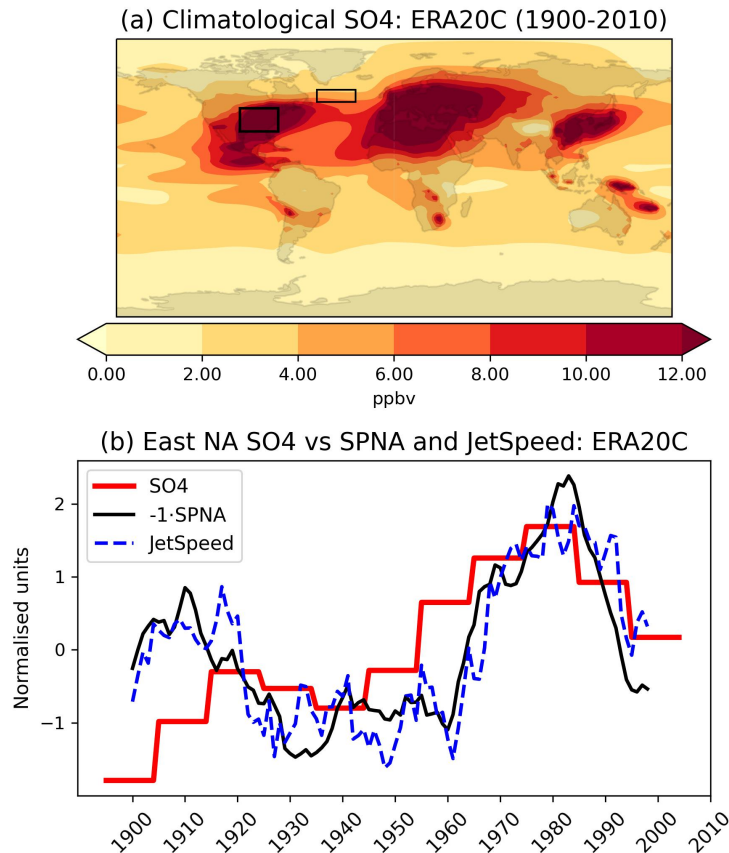


**Figure 12.** In (a): the climatological SO<sub>4</sub> emissions of ERA20C (in parts per billion by volume), which is the same as those in ASF20C and CSF20C. In (b), timeseries of the 10-year averaged ERA20C SPNA SSTs, jet speed and area-averaged East North American SO<sub>4</sub>. The sign of the SPNA timeseries has been flipped for visual convenience. In (a), the domain of the East North American region has been marked with a thick black box and the SPNA domain with a thin black box.

speed in Figure 12(b). The SO<sub>4</sub> timeseries matches both the SSTs and jet speed in the period 1940-2010, with a correlation of around 0.8. However, in the earlier period 1900-1940, the SO<sub>4</sub> emissions are anticorrelated with the SSTs and jet speed, with a correlation of around -0.3. Note that the CMIP5 aerosol forcing data is constant across each 10-year period, explaining the step-like quality of the SO<sub>4</sub> timeseries.

We conclude that while aerosol emissions over North America may have played a role in driving decadal SPNA variability, they are unlikely to explain the entire 20th century variability, especially in the early period when emissions are still very low. Similar conclusions were drawn in earlier work by Zhang et al. (2013). Note that the forecast models are able to capture the strong jet in this early period, despite the low aerosol emissions (Figure 1). If the aerosols are driving some of the SPNA variability, then this would be expected to lead to predictable shifts in the jet speed, as discussed in the present paper. It should

also be noted that an aerosol-induced cooling of North America would strengthen the land-sea contrast, which would also be expected to drive a stronger jet (Portal et al., 2022). It is unclear if such a change in land-sea contrast alone can generate decadal timescale forecast skill.

## 420 6.2 The role of the AMOC

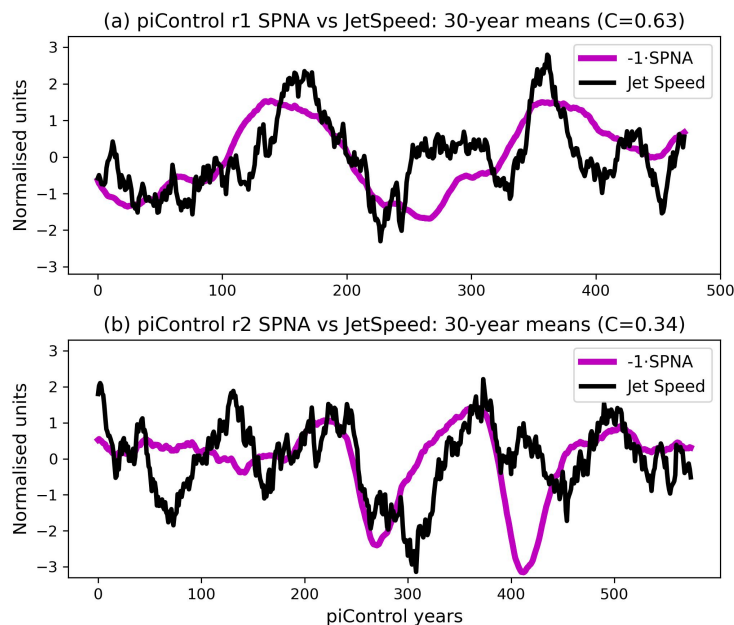


**Figure 13.** Timeseries of 30-year averages of the DJF SPNA SSTs (purple) and DJF jet speeds (black) in (a) the first EC-Earth3 pre-industrial control ensemble member, and (b) the same for the second ensemble member. The sign of the SPNA timeseries has been flipped for visual convenience. The value  $C$  in the titles indicates the correlation between the two timeseries. The timeseries have been normalised to have mean 0 and standard deviation 1.

To understand if the AMOC alone can drive SPNA-induced jet speed variability, we examine the two EC-Earth3 pre-industrial control simulations, which we refer to as piControl r1 and piControl r2. These simulations are particularly useful for assessing AMOC forcing, since they are known to exhibit large and striking centennial timescale AMOC oscillations (Meccia et al., 2022). The lack of any anthropogenic emissions means the associated variability in the SPNA will be entirely due to the AMOC.

Figure 13 shows 30-year running DJF means of SPNA SSTs vs JetSpeed for the two ensemble members. The centennial AMOC oscillations are clearly visible in the SPNA timeseries. The correlations obtained between the SPNA and JetSpeed are  $-0.63$  for the r1 member and  $-0.34$  for the r2 member. A 5% significance threshold using the same null hypothesis as before (modelling JetSpeed as white noise, SPNA with the Fourier phase shuffle method) is approximately  $\pm 0.5$ , implying that the r1 correlation is highly significant while the r2 is not.

We cannot directly compare the correlations from these free-running coupled simulations to the ensemble mean correlations of ASF20C. However, we note that if we concatenate back-to-back 5 ASF20C ensemble members, we get a timeseries of length  $5 \cdot 109 = 545$ , approximately the same length as the piControl members. By randomly drawing 5 ASF20C members, concatenating them, and computing the correlations between the resulting SPNA and JetSpeed timeseries, we can compare ASF20C and piControl in a like-for-like manner. If we carry out 1000 random such draws, we find that the expected ASF20C correlation is around -0.2 with a 95% confidence interval of approximately [-0.51, 0.18]. Almost identical results are obtained if using the CSF20C ensemble. This clearly suggests that the  $r_2$  correlation of -0.34 is perfectly consistent with the SPNA-JetSpeed link diagnosed in ASF20C/CSF20C. It also suggests that the  $r_1$  correlation of -0.63 is larger than expected, though not impossible, with a handful of concatenated ASF20C/CSF20C members producing correlations of around -0.6. Since the AMOC oscillations are particularly strong in the piControl runs, it is possible that this translates into SPNA-JetSpeed correlations which may be unrealistically large. The  $r_1$  member may also just be a random outlier.

Based on the above analysis we conclude that AMOC oscillations alone can in principle produce SPNA variations associated with an SPNA-JetSpeed link of the same strength as in the forecast models, even in the absence of any aerosol forcing. It is therefore natural to speculate that the AMOC is responsible for the coherent SPNA and jet speed variability seen in the early 20th century (Figure 12), and likely contributes to the variability later on as well.

## 7 Discussion

### 7.1 Other potential sources of skill

Our key argument for the importance of the SPNA can be understood as a conditional one: if one assumes that the skill comes from SSTs, then Figures 3 through 5 suggest that the SPNA is the responsible region. How reasonable is this assumption? In other words, could the skill originate from somewhere other than the ocean?

It is possible in principle that the skill comes from the stratosphere (Omriani et al., 2014), which has a decorrelation timescale of several months. However, the initial conditions of ASF20C (CSF20C) come from ERA20C (CERA20C), which only assimilates surface variables. Because these do not strongly constrain the stratosphere, the stratospheric variability in ERA20C is highly biased. Indeed, O'Reilly et al. (2019) found that the amplitude of the quasi-biennial oscillation (QBO) is substantially weaker in ERA20C compared to reanalysis products that assimilate a broader range of atmospheric observations. They also reported a greatly reduced downward propagation in ERA20C. O'Reilly et al. (2019) also considered the same ASF20C hindcasts and found that the seasonal timescale association between the QBO and the NAO was essentially zero, unlike in forecasts assimilating the stratosphere. We interpret this as evidence that there is limited scope for skill from stratospheric initial conditions in ASF20C/CSF20C. Another argument towards the stratosphere not driving the predictability was given in Simpson et al. (2018), which showed using reanalysis that the magnitude of stratospheric anomalies do not match those of the jet on decadal timescales. Note that while they only explicitly discussed March, their Figure B1 suggest similar conclusions would likely be drawn for DJF.

Besides the stratosphere, the remaining obvious candidates are ice and anthropogenic emissions such as carbon dioxide and aerosols. However, the impact of ice on decadal jet variability has been found to be small compared to SSTs (Peings and Magnusdottir, 2016; Ogawa et al., 2018; Liang et al., 2021). Furthermore, observations of ice are sparse and unevenly distributed prior to 1979, with obvious implications for the potential quality of the ice data used in the ASF20C boundary forcing files. As for anthropogenic emissions, the analysis in Simpson et al. (2018) showed that globally averaged emissions cannot explain the decadal variability of a closely related jet index. This leaves open the possible influence of local emissions. The most obvious way for such local emissions to alter the jet is *indirectly*, by altering the radiative forcing and hence surface temperatures. Such indirect forcings on the jet would manifest themselves as an apparent forcing from surface temperatures. While this could potentially include forcing from temperatures over land, the decorrelation timescale over land is much faster than for SSTs, making a decadal timescale forcing seem less likely. On the other hand, any indirect forcing via the SSTs would already be visible in Figures 3 and 4, which highlight the SPNA.

It is hard to exclude the possibility of a more direct impact of aerosols on the jet, e.g. due to an altering of the local radiative fluxes in the troposphere (as opposed to at the surface). Figure 12(a) shows that sulphate aerosol concentrations are small on the north side of the jet core, making a direct contribution from there seem less likely. There are more emissions centred around the jet core, so these could be playing a role. However, as pointed out in Section 6.1, aerosol emissions drop considerably prior to 1940 and become anticorrelated with the jet speed timeseries in the period 1900-1940, even as forecast skill remains high (Figure 12(b)). Such direct effects are therefore unlikely to explain all the observed skill.

While all these other potential sources of skill cannot be conclusively ruled out without targeted forecast experiments, we nevertheless conclude by process of elimination that there is strong evidence towards our assumption that the skill comes from the SSTs, and hence from the SPNA in particular.

## 7.2 The question of causality between ocean and atmosphere

There is an obvious question concerning the causality of the SPNA-JetSpeed link we have proposed, especially since SSTs in the SPNA are known to be particularly sensitive to forcing from the jet (Visbeck et al., 2003; Barrier et al., 2014; Ma et al., 2020). Are the correlations in Table 2 in fact just indicative of stochastic atmospheric forcing on the ocean? Here we discuss several lines of evidence which suggest that at least a considerable portion of the correlations are due to a genuine forcing from the ocean to the atmosphere.

The first key point is the apparent existence of skillful decadal forecasts. We have shown that the SPNA appears to be the only clear, common SST-based signal between reanalysis and the forecasts we have analysed. If the SPNA-JetSpeed correlations are mostly or entirely reflecting a causal influence of the atmosphere on the ocean then one seems forced to conclude that the decadal skill does not originate from the SSTs. This is problematic, given the discussion of Section 7.1.

Secondly, we remind the reader that ASF20C is uncoupled and uses prescribed boundary forcing, so correlations on interannual timescales in ASF20C cannot arise from a causal influence of the atmosphere on the SSTs in the model. While this is not true for CSF20C and DPLE, which are coupled, the fact that (i) the correlations they attain are entirely comparable to those of ASF20C, and (ii) all these correlations are explainable from the interannual link alone (Section 5.2), suggests that forcing

from the SSTs to the atmosphere constitutes a pragmatic common explanation for the correlations found in all three forecast models. An alternative explanation for the correlations seen in the uncoupled ASF20C would be the existence of a different source of skill, not related to SSTs, which influences both the jet and the SSTs (possibly via the jet). Since the correct SSTs are prescribed to ASF20C, such a common driver could result in correlations of the sort seen in Table 2. However, as before, the hypothetical existence of such a non-SST related driver is currently unfounded.

Figure 7 showed correlations between DJF SPNA and DJF temperatures/winds. If we rather correlate November SPNA anomalies against DJF temperatures/winds, we get a similar picture, albeit weaker in magnitude, especially for the winds: see Figure A2 in the SI. This suggests that the vertical heating is not purely coming from the adjustment of the jet itself, but also from processes induced by the SST anomalies. The fact that the heating associated with the SPNA peaks at the surface (Figure 7(a) and (c)), is also suggestive of SST driving. In general, replacing DJF SPNA SSTs with November averages leads to smaller but non-zero correlations of the same sign.

Another important reason for having a high prior for a causal influence from the SPNA are that several studies using idealised models and GCMs have demonstrated that SST anomalies can causally affect the jet (Palmer and Zhaobo, 1985; Deser et al., 2007; Hassanzadeh and Kuang, 2016; Baker et al., 2017, 2019). Of particular relevance is the recent work of Drews et al. (2023), who carried out pacemaker experiments which suggest that SSTs in the SPNA have a positive impact on decadal forecast skill. We also highlight Baker et al. (2017), who used a dry model to show that imposed heating anomalies modulate the speed of the eddy-driven jet by altering the meridional gradient around the jet core, making the causal pathway we propose here a plausible explanation for the observed decadal forecast skill. An important caveat here is the increasingly recognized role played by moist processes in determining the jet variability, which are not represented in such a dry model (Willison et al., 2013; Papritz and Spengler, 2015; Schemm, 2023; Fuchs et al., 2023). Note however that the results of Baker et al. (2017) are generally consistent with those in Baker et al. (2019) using a full moist GCM.

Finally, Simpson et al. (2018) showed that the DPLE forecasts can skillfully predict decadal SPNA SST variability, but fails to predict shorter timescale North Atlantic winds of an appreciable magnitude, strongly suggesting that decadal SPNA variability is not purely driven by stochastic atmospheric forcing. This was further corroborated by Yeager (2020), which found evidence that the SST skill has an abyssal origin. Consistent with this, quantitative estimates of the stochastic forcing in the coupled CSF20C hindcast, using methods such as the one described in Ma et al. (2020), were found to be very small in the SPNA region on decadal timescales, roughly an order of magnitude smaller than the observed SPNA-JetSpeed correlations (not shown).

To conclude, we consider it likely that there is a sufficient causal influence of the SPNA on the jet to explain the observed decadal skill. Unambiguously confirming this would, however, require performing expensive forecast experiments, such as rerunning the full ASF20C hindcast using boundary forcing files for which the SPNA SST variability has been eliminated.

### **7.3 Relationship with Atlantic Multidecadal Variability**

We have argued that the SPNA forces the NAO more or less instantaneously. How do our results relate to previous studies suggesting that the AMV forces the NAO, with the NAO response typically lagging the AMV by several years (Peings and



Magnusdottir, 2014b; Peings et al., 2016; Kwon et al., 2020)? We suggest that this apparent discrepancy is a result of three factors.

535 Firstly, while the AMV pattern on interannual timescales is the famous ‘horseshoe’ pattern, the pattern largely collapses to a signal confined to the SPNA after performing decadal timescale smoothing (Delworth et al., 2017; Simpson et al., 2018). This suggests that as far as decadal atmospheric variability is concerned, the SPNA is more relevant than the ‘horseshoe’ pattern. The importance of this region has been highlighted previously (Gastineau and Frankignoul, 2015; Woollings et al., 2015; Ortega et al., 2017; Delworth et al., 2017; Wills et al., 2019).

540 Secondly, anomalies in the SPNA (the northern part of the ‘horseshoe’) are observed to lead anomalies in the tropical Atlantic (the southern part of the ‘horseshoe’) by around 2 years (Zhang, 2007). It is likely that this propagation of anomalies takes place both via subsurface ocean dynamics and coupling with the atmosphere (Zhang et al., 2019). This means that performing analysis based on the standard AMV ‘horseshoe’ pattern is mixing together different processes happening on different timescales. Since the SPNA anomalies arise first, restricting attention to these might be expected to give a clearer picture and better highlight causal pathways from the ocean to the atmosphere. This argument has also recently been made by Wills et al. (2019). Note that this second point is presumably related to the first, since taking decadal averages would  
545 be expected to remove the shorter timescale signals associated with propagation of SST anomalies along the ‘horseshoe’ and processes operating at much slower timescales, such as those associated with deep convection in the Labrador sea. This argument was also made in Delworth et al. (2017).

Thirdly, the reverse impact of the NAO on the AMV has also been noted to operate on both fast and slow multi-year timescales (Ma et al., 2020; Khatri et al., 2022), introducing additional lags to the coupled AMV-NAO system.

550 We therefore suggest that the apparent existence of an NAO response lagging the AMV by several years is, in fact, largely reflecting the existence of an essentially instantaneous atmospheric response to the SPNA, with the multi-year lag being an artefact of using an AMV index which averages across several different processes. This is further supported by Figure 11. The AMV-JetSpeed lag-correlations (red curve) show a peak at 7-15 years (depending on smoothing choices) when the AMV leads, reproducing what is found using the NAO index (Peings and Magnusdottir, 2014b; Peings et al., 2016). When the SPNA index  
555 is used, this lag vanishes, with correlations now peaking at lag 0.

#### **7.4 Why is the jet latitude not predictable?**

Several studies have argued that an AMV-driven NAO response involves a shift in both the strength and location of the storm track and/or baroclinic region (Msadek et al., 2011; Peings and Magnusdottir, 2014a; Frankignoul et al., 2015; Peings et al., 2016; Ortega et al., 2017). Such systematic latitudinal shifts in the storm track/baroclinicity, and hence the eddies, would be  
560 expected to manifest as predictable latitudinal shifts in the eddy-driven jet itself. However, as discussed in Section 3, there is no decadal predictability of the latitude of the jet in ASF20C, CSF20C or DPLE. This suggests that on decadal timescales, the eddies are randomly distributed around their mean position, and that the mechanism driving predictable jet variability does not essentially depend on latitudinal shifts in the storm track. Rather, such predictable changes appear to be more clearly related

to the direct constraint of thermal wind balance along with an *intensification* of the storm track. This is fully consistent with  
565 Woollings et al. (2015), who highlighted the contrasting nature of forced shifts to the latitude and speed of the jet.

Of course, it cannot be ruled out that SST anomalies in the SPNA, or indeed elsewhere, force shifts in the latitude of the  
jet in the real world that are simply not captured by the forecast models we considered. However, until predictability has been  
established it does not seem possible to reject the null hypothesis that decadal variability in the jet latitude is chaotic and  
unpredictable. Indeed, the inconsistent latitudinal response in multimodel studies such as Ruggieri et al. (2021) lends concrete  
570 evidence for such inherent chaos. Further evidence for this is given in Figure A3 of the SI, which repeats the procedure of  
Section 4 to search for potential sources of jet latitude skill in ASF20C. This shows that there are no regions of significant  
SST-jet latitude correlations common to both ERA20C and ASF20C, consistent with the lack of jet latitude predictability.

It is also possible that biases in the climatological jet latitude (i.e., in the model mean state) of the forecast models are  
contributing to the apparent lack of jet latitude predictability. The sensitivity analysis of Baker et al. (2017) showed that the  
575 response of the jet latitude to thermal forcing changes sign abruptly around the jet core, while the response of the jet speed is  
more uniform across the jet. The accurate response of a model jet to a given SST anomaly may therefore differ dramatically  
based on its climatological position. This could go some way to explaining the inconsistent jet latitude response in multimodel  
studies such as Ruggieri et al. (2021).

## 8 Conclusions

580 We briefly summarise the main results and arguments.

1. Decadal forecast skill of the winter NAO appears to be entirely due to the decadal predictability of the speed of the North  
Atlantic jet. There is no apparent predictability of decadal variations in the latitude of the jet, even in seasonal hindcasts  
with prescribed SSTs (Figures 1 and 2).
2. Initialised seasonal hindcasts can skillfully reproduce decadal variations in jet speed all the way back to 1900, and match  
585 the behaviour of a genuine decadal forecast in the period 1954-2010. This justifies using such seasonal hindcasts to  
diagnose decadal forecast signals using the full period 1900-2010, effectively doubling the available years compared to  
existing decadal forecasts. In addition, this strongly suggests that the decadal forecast signals are already fully present  
and visible on interannual timescales.
3. The only clear source of an interannual-to-decadal jet speed signal coming from SSTs, common to reanalysis and fore-  
590 casts, is the SPNA region (Figures 3 and 4). SSTs in this region enjoy large and statistically significant correlations with  
the jet speed, which we argue are due at least in part to a causal link from the ocean to the atmosphere (Figure 6). We  
also show that all of the decadal SPNA-JetSpeed link in the forecast models, along with the associated forecast skill, can  
be explained by a small but consistent seasonal timescale forcing from the SSTs (Figures 10 and 11).

595 4. The pathway from SPNA SSTs to the jet speed is argued to be tropospheric in nature: the surface heating anomaly extends relatively deeply into the troposphere (Figure 7) and is optimally situated to perturb the jet speed both by direct adjustments consistent with thermal wind balance and subsequent reinforcements by the eddies.

5. Sulphate aerosol emissions in North America may explain part of the 20th century covariability of the SPNA and jet speed, but do not explain the early 20th century (Figure 12). AMOC oscillations alone are shown to be capable of inducing SST shifts of strength comparable to those connected with jet speed variability (Figure 13).

600 Note that the importance of the SPNA in driving predictable decadal jet variability was emphasised in Simpson et al. (2018) using a different metric of North Atlantic jet variability in March. Our work here is clearly closely related and was directly inspired by theirs.

There are several shortcomings to our analysis, chief of which is the fact that we have only studied two independent forecast models. However, Marcheggiani et al. (2023) have recently analysed the decadal forecasts used in Smith et al. (2019) and  
605 found that the jet speed is much more predictable than the jet latitude. They also linked the predictability to North Atlantic SSTs, thereby reinforcing two of our key conclusions using independent data. Our argument that the stratosphere is unlikely to be relevant due to the initialisation biases of the seasonal hindcasts may also be flawed, and it would be of interest to examine the role of the stratosphere more closely. We also interpreted the similar jet speed correlations in ASF20C/CSF20C and DPLE as evidence that the mechanisms involved are the same for these data sets. However, it may be that ASF20C/CSF20C obtain  
610 most of their ‘skill’ from the initialisation (lag 0), while DPLE obtains most of its skill from representing slower frequency coupled processes better (lags > 0). If so, conclusions drawn using ASF20C/CSF20C may not carry over to a genuine forecast context. Nevertheless, our findings have some important implications.

To begin with, we have reinforced the conclusion of earlier studies such as Baker et al. (2017) that the speed and latitude of the jet should be considered separately, and that the use of indices like the NAO (which amalgamate the two) may be  
615 misleading. Our finding that the decadal averaged jet speed is predictable while the latitude is not stands in amusing contrast to work on *seasonal* forecasts, which suggest the opposite picture of a predictable latitude and unpredictable speed (Parker et al., 2019). This reinforces the analysis of Woollings et al. (2015), who showed that the nature of forced jet variability differs depending on the timescale. On interannual timescales, the variability is dominated by the jet latitude, in turn associated with meridional shifts in the transient eddies and location of blocking. On decadal timescales, the variability is dominated by the jet  
620 speed, in turn associated with changes both to the *strength* of the eddy forcing and to the occurrence of transient Rossby wave breaking on both sides of the jet. Our analysis corroborates the speculation in Woollings et al. (2015) that this may result in the nature and sources of predictability being different on the two timescales. In particular, our results are consistent with the following hypothetical view of the jet variability:

(a) On seasonal timescales the forcing from the SPNA is too small to be easily visible (resulting in the appearance of no jet  
625 speed skill), with jet latitude skill arising from accurately predicting meridional shifts in the eddies;

(b) On decadal timescales the eddies are varying essentially chaotically around their climatological position (resulting in no jet latitude predictability), but their intensity can vary predictably depending on the underlying SPNA SSTs, which strengthen or weaken the meridional temperature gradient.

A novelty of our work is the use of the initialised 20th century seasonal hindcast products ASF20C and CSF20C. While  
630 Parker et al. (2019) considered the fast and slow variability of the jet speed and latitude in ASF20C, the possibility of utilising these hindcasts to study the mechanisms underpinning decadal predictability seems to have been overlooked. The fact that ASF20C covers the entire 20th century, is reinitialised every year, and is uncoupled, are all highly attractive properties for simplifying analysis which we made extensive use of. We believe that ASF20C may be similarly beneficial for the study of decadal predictability in many other contexts.

635 Finally, we add to a growing body of literature suggesting that the SPNA is the main source of North Atlantic jet forcing on decadal timescales, and that the use of a larger AMV or AMO pattern might be counterproductive for questions of predictability by mixing together different mechanisms and timescales. We have shown that the SST variability in the SPNA driving predictable jet speed shifts can in principle be due to both the AMOC and aerosol emissions, and it seems likely that the observed 20th century variability is a result of both of these. We do not shed further light in this study on the ‘signal-to-noise paradox’,  
640 but our results suggest that it may be particularly interesting to examine how well forecast models simulate fast timescale atmosphere-ocean coupling in the SPNA region. This is a natural avenue for future work.

*Data availability.* ASF20C and CSF20C data is freely available on CEDA (Weisheimer, 2020). ERA20C data is freely available via ECMWF at <https://apps.ecmwf.int/datasets/data/era20c-daily/levtype=sfc/type=an/>. DPLE data is available via the Earth System Grid Federation (Yeager, 2018).

645 *Author contributions.* KS led the writing of the manuscript and carried out the majority of the data analysis. PR and PD contributed data analysis related to idealised model results and the role of the AMOC in the pre-industrial CMIP6 simulations; aided with literature review; and helped interpret results. TW aided interpretation of results and provided expert guidance on physical mechanisms. IRS helped in the procurement and analysis of DPLE model data and interpretation of the results.

*Competing interests.* We declare that there are no competing interests.

650 *Acknowledgements.* KS was funded by a Thomas Philips and Jocelyn Keene Junior Research Fellowship at Jesus College, Oxford. PR acknowledges the use of computational resources from the parallel computing cluster of the Open Physics Hub (<https://site.unibo.it/openphysicshub/en>) at the Department of Physics and Astronomy of the University of Bologna. IRS was supported by the National Center for Atmospheric Research which is a major facility sponsored by the National Science Foundation under the Cooperative Agreement 1852977.

## References

- 655 Athanasiadis, P. J., Yeager, S., Kwon, Y.-O., Bellucci, A., Smith, D. W., and Tibaldi, S.: Decadal predictability of North Atlantic blocking and the NAO, *NPJ Climate and Atmospheric Science*, 3, 1–10, 2020.
- Baker, H. S., Woollings, T., and Mbengue, C.: Eddy-driven jet sensitivity to diabatic heating in an idealized GCM, *Journal of Climate*, 30, 6413–6431, 2017.
- 660 Baker, H. S., Woollings, T., Forest, C. E., and Allen, M. R.: The linear sensitivity of the North Atlantic Oscillation and eddy-driven jet to SSTs, *Journal of Climate*, 32, 6491–6511, 2019.
- Barrier, N., Cassou, C., Deshayes, J., and Treguier, A.-M.: Response of North Atlantic Ocean circulation to atmospheric weather regimes, *Journal of Physical Oceanography*, 44, 179–201, 2014.
- Bellomo, K., Murphy, L. N., Cane, M. A., Clement, A. C., and Polvani, L. M.: Historical forcings as main drivers of the Atlantic multidecadal variability in the CESM large ensemble, *Climate Dynamics*, 50, 3687–3698, 2018.
- 665 Bjerknes, J.: Atlantic air-sea interaction, in: *Advances in geophysics*, vol. 10, pp. 1–82, Elsevier, 1964.
- Booth, B. B., Dunstone, N. J., Halloran, P. R., Andrews, T., and Bellouin, N.: Aerosols implicated as a prime driver of twentieth-century North Atlantic climate variability, *Nature*, 484, 228–232, 2012.
- Bracegirdle, T. J.: Early-to-Late Winter 20th Century North Atlantic Multidecadal Atmospheric Variability in Observations, CMIP5 and CMIP6, *Geophysical Research Letters*, 49, e2022GL098 212, 2022.
- 670 Clement, A., Bellomo, K., Murphy, L. N., Cane, M. A., Mauritsen, T., Rädel, G., and Stevens, B.: The Atlantic Multidecadal Oscillation without a role for ocean circulation, *Science*, 350, 320–324, 2015.
- Danabasoglu, G., Bates, S. C., Briegleb, B. P., Jayne, S. R., Jochum, M., Large, W. G., Peacock, S., and Yeager, S. G.: The CCSM4 ocean component, *Journal of Climate*, 25, 1361–1389, 2012.
- Davini, P., von Hardenberg, J., and Corti, S.: Tropical origin for the impacts of the Atlantic multidecadal variability on the Euro-Atlantic 675 climate, *Environmental Research Letters*, 10, 094 010, 2015.
- Dell’Aquila, A., Corti, S., Weisheimer, A., Hersbach, H., Peubey, C., Poli, P., Berrisford, P., Dee, D., and Simmons, A.: Benchmarking Northern Hemisphere midlatitude atmospheric synoptic variability in centennial reanalysis and numerical simulations, *Geophysical Research Letters*, 43, 5442–5449, 2016.
- Delworth, T., Manabe, S., and Stouffer, R. J.: Interdecadal variations of the thermohaline circulation in a coupled ocean-atmosphere model, 680 *Journal of Climate*, 6, 1993–2011, 1993.
- Delworth, T. L., Zeng, F., Zhang, L., Zhang, R., Vecchi, G. A., and Yang, X.: The Central Role of Ocean Dynamics in Connecting the North Atlantic Oscillation to the Extratropical Component of the Atlantic Multidecadal Oscillation, *Journal of Climate*, 30, 3789 – 3805, <https://doi.org/10.1175/JCLI-D-16-0358.1>, 2017.
- Deser, C. and Phillips, A. S.: Defining the internal component of Atlantic multidecadal variability in a changing climate, *Geophysical 685 Research Letters*, 48, e2021GL095 023, 2021.
- Deser, C., Tomas, R. A., and Peng, S.: The Transient Atmospheric Circulation Response to North Atlantic SST and Sea Ice Anomalies, *Journal of Climate*, 20, 4751 – 4767, <https://doi.org/10.1175/JCLI4278.1>, 2007.
- Döscher, R., Acosta, M., Alessandri, A., Anthoni, P., Arsouze, T., Bergman, T., Bernardello, R., Boussetta, S., Caron, L.-P., Carver, G., et al.: The EC-Earth3 earth system model for the coupled model intercomparison project 6, *Geoscientific Model Development*, 15, 2973–3020, 690 2022.

- Drews, A., Schmith, T., Yang, S., Olsen, S., Tian, T., Devilliers, M., Wang, Y., and Keenlyside, N.: Role of the subpolar North Atlantic region in skillful climate predictions for high northern latitudes: A pacemaker experiment, EGU General Assembly 2023, Vienna, Austria, 24–28 Apr 2023, EGU23-13375, <https://doi.org/https://doi.org/10.5194/egusphere-egu23-13375>, 2023.
- Ebisuzaki, W.: A method to estimate the statistical significance of a correlation when the data are serially correlated, *Journal of climate*, 10, 2147–2153, 1997.
- Fichefet, T. and Maqueda, M. M.: Sensitivity of a global sea ice model to the treatment of ice thermodynamics and dynamics, *Journal of Geophysical Research: Oceans*, 102, 12 609–12 646, 1997.
- Frankignoul, C., Gastineau, G., and Kwon, Y.-O.: Wintertime Atmospheric Response to North Atlantic Ocean Circulation Variability in a Climate Model, *Journal of Climate*, 28, 7659 – 7677, <https://doi.org/10.1175/JCLI-D-15-0007.1>, 2015.
- 700 Fuchs, D., Sherwood, S. C., Waugh, D., Dixit, V., England, M. H., Hwong, Y.-L., and Geoffroy, O.: Midlatitude jet position spread linked to atmospheric convective types, *Journal of Climate*, 36, 1247–1265, 2023.
- Gastineau, G. and Frankignoul, C.: Influence of the North Atlantic SST Variability on the Atmospheric Circulation during the Twentieth Century, *Journal of Climate*, 28, 1396 – 1416, <https://doi.org/10.1175/JCLI-D-14-00424.1>, 2015.
- Hassanzadeh, P. and Kuang, Z.: The linear response function of an idealized atmosphere. Part I: Construction using Green’s functions and applications, *Journal of the Atmospheric Sciences*, 73, 3423–3439, 2016.
- 705 Hasselmann, K.: Stochastic climate models part I. Theory, *tellus*, 28, 473–485, 1976.
- Hunke, E. C., Lipscomb, W. H., Turner, A. K., Jeffery, N., and Elliott, S.: Cice: the los alamos sea ice model documentation and software user’s manual version 4.1 la-cc-06-012, T-3 Fluid Dynamics Group, Los Alamos National Laboratory, 675, 500, 2010.
- Hurrell, J. W., Holland, M. M., Gent, P. R., Ghan, S., Kay, J. E., Kushner, P. J., Lamarque, J.-F., Large, W. G., Lawrence, D., Lindsay, K., et al.: The community earth system model: a framework for collaborative research, *Bulletin of the American Meteorological Society*, 94, 1339–1360, 2013.
- 710 Johnson, S. J., Stockdale, T. N., Ferranti, L., Balmaseda, M. A., Molteni, F., Magnusson, L., Tietsche, S., Decremmer, D., Weisheimer, A., Balsamo, G., et al.: SEAS5: the new ECMWF seasonal forecast system, *Geoscientific Model Development*, 12, 1087–1117, 2019.
- Judt, F.: Atmospheric predictability of the tropics, middle latitudes, and polar regions explored through global storm-resolving simulations, *Journal of the Atmospheric Sciences*, 77, 257–276, 2020.
- 715 Kay, J. E., Deser, C., Phillips, A., Mai, A., Hannay, C., Strand, G., Arblaster, J. M., Bates, S., Danabasoglu, G., Edwards, J., et al.: The Community Earth System Model (CESM) large ensemble project: A community resource for studying climate change in the presence of internal climate variability, *Bulletin of the American Meteorological Society*, 96, 1333–1349, 2015.
- Khatri, H., Williams, R. G., Woollings, T., and Smith, D. M.: Fast and slow subpolar ocean responses to the North Atlantic Oscillation: Thermal and dynamical changes, *Geophysical Research Letters*, 49, e2022GL101 480, 2022.
- 720 Kim, W. M., Yeager, S., Chang, P., and Danabasoglu, G.: Low-frequency North Atlantic climate variability in the Community Earth System Model large ensemble, *Journal of Climate*, 31, 787–813, 2018.
- Kravtsov, S.: Pronounced differences between observed and CMIP5-simulated multidecadal climate variability in the twentieth century, *Geophysical Research Letters*, 44, 5749–5757, 2017.
- 725 Kushnir, Y.: Interdecadal variations in North Atlantic sea surface temperature and associated atmospheric conditions, *Journal of Climate*, 7, 141–157, 1994.
- Kushnir, Y., Robinson, W., Bladé, I., Hall, N., Peng, S., and Sutton, R.: Atmospheric GCM response to extratropical SST anomalies: Synthesis and evaluation, *Journal of Climate*, 15, 2233–2256, 2002.

- 730 Kwon, Y.-O., Seo, H., Ummerhofer, C. C., and Joyce, T. M.: Impact of multidecadal variability in Atlantic SST on winter atmospheric blocking, *Journal of Climate*, 33, 867–892, 2020.
- Laloyaux, P., de Boissesson, E., Balmaseda, M., Bidlot, J.-R., Broennimann, S., Buizza, R., Dalhgren, P., Dee, D., Haimberger, L., Hersbach, H., et al.: CERA-20C: A coupled reanalysis of the twentieth century, *Journal of Advances in Modeling Earth Systems*, 10, 1172–1195, 2018.
- 735 Lamarque, J.-F., Bond, T. C., Eyring, V., Granier, C., Heil, A., Klimont, Z., Lee, D., Liousse, C., Mieville, A., Owen, B., et al.: Historical (1850–2000) gridded anthropogenic and biomass burning emissions of reactive gases and aerosols: methodology and application, *Atmospheric Chemistry and Physics*, 10, 7017–7039, 2010.
- Liang, Y.-C., Frankignoul, C., Kwon, Y.-O., Gastineau, G., Manzini, E., Danabasoglu, G., Suo, L., Yeager, S., Gao, Y., Attema, J. J., et al.: Impacts of Arctic sea ice on cold season atmospheric variability and trends estimated from observations and a multimodel large ensemble, *Journal of Climate*, 34, 8419–8443, 2021.
- 740 Ma, L., Woollings, T., Williams, R. G., Smith, D., and Dunstone, N.: How does the winter jet stream affect surface temperature, heat flux, and sea ice in the North Atlantic?, *Journal of Climate*, 33, 3711–3730, 2020.
- Madec, G. and the NEMO team: NEMO ocean engine version 3.6 stable, Note du Pôle de modélisation de l’Institut Pierre-Simon Laplace, 27, 2016.
- 745 Marcheggiani, A., Robson, J., Monerie, P.-A., Bracegirdle, T. J., and Smith, D.: Decadal Predictability of the North Atlantic Eddy-Driven Jet in Winter, *Geophysical Research Letters*, 50, e2022GL102071, 2023.
- Meccia, V. L., Fuentes-Franco, R., Davini, P., Bellomo, K., Fabiano, F., Yang, S., and von Hardenberg, J.: Internal multi-centennial variability of the Atlantic Meridional Overturning Circulation simulated by EC-Earth3, *Climate Dynamics*, pp. 1–18, 2022.
- Msadek, R., Frankignoul, C., and Li, L. Z.: Mechanisms of the atmospheric response to North Atlantic multidecadal variability: A model study, *Climate dynamics*, 36, 1255–1276, 2011.
- 750 Ogawa, F., Keenlyside, N., Gao, Y., Koenigk, T., Yang, S., Suo, L., Wang, T., Gastineau, G., Nakamura, T., Cheung, H. N., et al.: Evaluating impacts of recent Arctic sea ice loss on the northern hemisphere winter climate change, *Geophysical Research Letters*, 45, 3255–3263, 2018.
- Omrani, N.-E., Keenlyside, N. S., Bader, J., and Manzini, E.: Stratosphere key for wintertime atmospheric response to warm Atlantic decadal conditions, *Climate Dynamics*, 42, 649–663, 2014.
- 755 O’Reilly, C. H., Weisheimer, A., Woollings, T., Gray, L. J., and MacLeod, D.: The importance of stratospheric initial conditions for winter North Atlantic Oscillation predictability and implications for the signal-to-noise paradox, *Quarterly Journal of the Royal Meteorological Society*, 145, 131–146, 2019.
- Ortega, P., Robson, J., Sutton, R. T., and Andrews, M. B.: Mechanisms of decadal variability in the Labrador Sea and the wider North Atlantic in a high-resolution climate model, *Climate Dynamics*, 49, 2625–2647, 2017.
- 760 O’Reilly, C. H., Zanna, L., and Woollings, T.: Assessing external and internal sources of Atlantic multidecadal variability using models, proxy data, and early instrumental indices, *Journal of Climate*, 32, 7727–7745, 2019.
- Palmer, T. and Zhaobo, S.: A modelling and observational study of the relationship between sea surface temperature in the north-west Atlantic and the atmospheric general circulation, *Quarterly Journal of the Royal Meteorological Society*, 111, 947–975, 1985.
- Papritz, L. and Spengler, T.: Analysis of the slope of isentropic surfaces and its tendencies over the North Atlantic, *Quarterly Journal of the*  
765 *Royal Meteorological Society*, 141, 3226–3238, 2015.

- Parker, T., Woollings, T., Weisheimer, A., O'Reilly, C., Baker, L., and Shaffrey, L.: Seasonal Predictability of the Winter North Atlantic Oscillation From a Jet Stream Perspective, *Geophysical Research Letters*, 46, 10 159–10 167, <https://doi.org/10.1029/2019GL084402>, 2019.
- Peings, Y. and Magnusdottir, G.: Response of the Wintertime Northern Hemisphere Atmospheric Circulation to Current and Projected Arctic Sea Ice Decline: A Numerical Study with CAM5, *Journal of Climate*, 27, 244 – 264, <https://doi.org/10.1175/JCLI-D-13-00272.1>, 2014a.
- Peings, Y. and Magnusdottir, G.: Forcing of the wintertime atmospheric circulation by the multidecadal fluctuations of the North Atlantic Ocean, *Environmental Research Letters*, 9, 034 018, 2014b.
- Peings, Y. and Magnusdottir, G.: Wintertime atmospheric response to Atlantic multidecadal variability: Effect of stratospheric representation and ocean–atmosphere coupling, *Climate dynamics*, 47, 1029–1047, 2016.
- 775 Peings, Y., Simpkins, G., and Magnusdottir, G.: Multidecadal fluctuations of the North Atlantic Ocean and feedback on the winter climate in CMIP5 control simulations, *Journal of Geophysical Research: Atmospheres*, 121, 2571–2592, 2016.
- Poli, P., Hersbach, H., Tan, D., Dee, D., Thépaut, J.-N., Simmons, A., Peubey, C., Laloyaux, P., Komori, T., Berrisford, P., and Dragani, R.: The data assimilation system and initial performance evaluation of the ECMWF pilot reanalysis of the 20th-century assimilating surface observations only (ERA-20C), ERA report series, 2013.
- 780 Portal, A., Pasquero, C., D'andrea, F., Davini, P., Hamouda, M. E., and Rivière, G.: Influence of Reduced Winter Land–Sea Contrast on the Midlatitude Atmospheric Circulation, *Journal of Climate*, 35, 2637–2651, 2022.
- Rayner, N. A., Parker, D. E., Horton, E. B., Folland, C. K., Alexander, L. V., Rowell, D. P., Kent, E. C., and Kaplan, A.: Global analyses of sea surface temperature, sea ice, and night marine air temperature since the late nineteenth century, *Journal of Geophysical Research D: Atmospheres*, 2003.
- 785 Robson, J., Menary, M. B., Sutton, R. T., Mecking, J., Gregory, J. M., Jones, C., Sinha, B., Stevens, D. P., and Wilcox, L. J.: The role of anthropogenic aerosol forcing in the 1850–1985 strengthening of the AMOC in CMIP6 historical simulations, *Journal of Climate*, 35, 3243–3263, 2022.
- Ruggieri, P., Bellucci, A., Nicolí, D., Athanasiadis, P. J., Gualdi, S., Cassou, C., Castruccio, F., Danabasoglu, G., Davini, P., Dunstone, N., et al.: Atlantic multidecadal variability and North Atlantic jet: a multimodel view from the decadal climate prediction project, *Journal of*
- 790 *Climate*, 34, 347–360, 2021.
- Scaife, A. A. and Smith, D.: A signal-to-noise paradox in climate science, *npj Climate and Atmospheric Science*, 1, 28, 2018.
- Schemm, S.: Toward Eliminating the Decades-Old “Too Zonal and Too Equatorward” Storm-Track Bias in Climate Models, *Journal of Advances in Modeling Earth Systems*, 15, e2022MS003 482, 2023.
- Shepherd, T. G.: Bringing physical reasoning into statistical practice in climate-change science, *Climatic Change*, 169, 2, 2021.
- 795 Simpson, I. R., Deser, C., McKinnon, K. A., and Barnes, E. A.: Modeled and Observed Multidecadal Variability in the North Atlantic Jet Stream and Its Connection to Sea Surface Temperatures, *Journal of Climate*, 31, 8313 – 8338, <https://doi.org/10.1175/JCLI-D-18-0168.1>, 2018.
- Smith, D., Eade, R., Scaife, A. A., Caron, L.-P., Danabasoglu, G., DelSole, T., Delworth, T., Doblas-Reyes, F., Dunstone, N., Hermanson, L., et al.: Robust skill of decadal climate predictions, *Npj Climate and Atmospheric Science*, 2, 1–10, 2019.
- 800 Visbeck, M., Chassignet, E. P., Curry, R. G., Delworth, T. L., Dickson, R. R., and Krahnmann, G.: The ocean's response to North Atlantic Oscillation variability, *Geophysical Monograph-American Geophysical Union*, 134, 113–146, 2003.
- Wang, X., Li, J., Sun, C., and Liu, T.: NAO and its relationship with the Northern Hemisphere mean surface temperature in CMIP5 simulations, *Journal of Geophysical Research: Atmospheres*, 122, 4202–4227, 2017.



- 805 Weisheimer, A., Schaller, N., O'Reilly, C., MacLeod, D. A., and Palmer, T.: Atmospheric seasonal forecasts of the twentieth century: multi-decadal variability in predictive skill of the winter North Atlantic Oscillation (NAO) and their potential value for extreme event attribution, *Quarterly Journal of the Royal Meteorological Society*, <https://doi.org/10.1002/qj.2976>, 2017.
- Weisheimer, A., Befort, D. J., MacLeod, D., Palmer, T., O'Reilly, C., and Strømme, K.: Seasonal forecasts of the twentieth century, *Bulletin of the American Meteorological Society*, 101, E1413–E1426, 2020.
- 810 Weisheimer, A.; O'Reilly, C.: Initialised seasonal forecast of the 20th Century., <https://catalogue.ceda.ac.uk/uuid/6e1c3df49f644a0f812818080bed5e45>, 2020.
- Willison, J., Robinson, W. A., and Lackmann, G. M.: The importance of resolving mesoscale latent heating in the North Atlantic storm track, *Journal of the Atmospheric Sciences*, 70, 2234–2250, 2013.
- Wills, R. C., Armour, K. C., Battisti, D. S., and Hartmann, D. L.: Ocean–atmosphere dynamical coupling fundamental to the Atlantic multidecadal oscillation, *Journal of Climate*, 32, 251–272, 2019.
- 815 Woollings, T., Hannachi, A., and Hoskins, B.: Variability of the North Atlantic eddy-driven jet stream, *Quarterly Journal of the Royal Meteorological Society*, 136, 856–868, <https://doi.org/10.1002/qj.625>, 2010.
- Woollings, T., Czuchnicki, C., and Franzke, C.: Twentieth century North Atlantic jet variability, *Quarterly Journal of the Royal Meteorological Society*, 140, 783–791, <https://doi.org/10.1002/qj.2197>, 2014.
- 820 Woollings, T., Franzke, C., Hodson, D., Dong, B., Barnes, E. A., Raible, C., and Pinto, J.: Contrasting interannual and multidecadal NAO variability, *Climate Dynamics*, 45, 539–556, 2015.
- Yeager, S.: Decadal Prediction Large Ensemble Project, <https://doi.org/10.5065/D6DR2T8H>, 2018.
- Yeager, S.: The abyssal origins of North Atlantic decadal predictability, *Climate Dynamics*, 55, 2253–2271, 2020.
- Yeager, S., Danabasoglu, G., Rosenbloom, N., Strand, W., Bates, S., Meehl, G., Karspeck, A., Lindsay, K., Long, M., Teng, H., et al.: Predicting near-term changes in the earth system: a large ensemble of initialized decadal prediction simulations using the community earth system model, *Bulletin of the American Meteorological Society*, 99, 1867–1886, 2018.
- 825 Zhang, R.: Anticorrelated multidecadal variations between surface and subsurface tropical North Atlantic, *Geophysical Research Letters*, 34, 2007.
- Zhang, R., Delworth, T. L., Sutton, R., Hodson, D. L., Dixon, K. W., Held, I. M., Kushnir, Y., Marshall, J., Ming, Y., Msadek, R., et al.: Have aerosols caused the observed Atlantic multidecadal variability?, *Journal of the Atmospheric Sciences*, 70, 1135–1144, 2013.
- 830 Zhang, R., Sutton, R., Danabasoglu, G., Kwon, Y.-O., Marsh, R., Yeager, S. G., Amrhein, D. E., and Little, C. M.: A review of the role of the Atlantic meridional overturning circulation in Atlantic multidecadal variability and associated climate impacts, *Reviews of Geophysics*, 57, 316–375, 2019.